

Tropospheric Ozone Production Pathways with Detailed Chemical Mechanisms

Dissertation zur Erlangung des akademischen Grades
des Doktors der Naturwissenschaften
am Fachbereich Geowissenschaften
an der Freien Universität Berlin

Vorgelegt von
Jane Coates
im Juli 2016



1. Gutachter: Prof. Dr. Mark Lawrence
2. Gutachter: Prof. Dr. Peter Builtjes

Abstract

Acknowledgements

Table of Contents

1	Introduction	1
1.1	Ozone	2
1.2	Ozone Chemistry	3
1.2.1	VOC and NOx Chemistry	8
1.2.2	Representing Atmospheric Chemistry in Models	9
1.3	Emissions of Ozone Precursors	9
1.3.1	NOx	9
1.3.2	VOCs	10
1.3.3	Representing VOC Emissions in Models	12
1.4	Effects of Meteorology on Ozone Production	14
1.5	Research Questions	16
2	Methodology	21
2.1	Air Quality Modelling	21
2.1.1	Model Description and Setup	23
2.2	Chemical Mechanisms	24
2.2.1	Near-Explicit Chemical Mechanisms	25
2.2.2	Lumped Intermediate Chemical Mechanisms	27

2.2.3	Lumped Molecule Chemical Mechanisms	29
2.2.4	Lumped Structure Chemical Mechanisms	33
2.3	Using the Chemical Mechanisms in MECCA	34
3	Presentation of Papers	37
3.1	Paper 1: A comparison of chemical mechanisms using tagged ozone production potential (TOPP) analysis	37
3.2	Paper 2:	39
3.3	Paper 3:	39
4	Overall Discussion and Conclusions	41
5	Summary and Zusammenfassung	43
	References	45
6	Paper 1: A comparison of chemical mechanisms using tagged ozone production potential (TOPP) analysis	55
7	Paper 2:	71
8	Paper 3:	73
9	Publication List	75
	Appendix	77

List of Tables

1.1	SNAP sectors in the TNO_MACCIII	13
1.2	Influence of meteorological variables on ozone production	14
2.1	General settings used for MECCA box model in this study	24
2.2	Chemical mechanisms used in the study.	25
2.3	Summary of the CRI v2 and its five reduced variants.	29
2.4	Explicitness of each of the lumped-molecule chemical mechanisms listed in Table 2.2	30
2.5	Carbon bonds and mechanism species represented in CBM-IV and CB05.	33

List of Figures

1.1	Methane degradation pathways	18
1.2	Schematic of general secondary degradation of VOCs	19
1.3	Ozone mixing ratios as a function of NO _x and VOC	19
2.1	Flowchart of VOC degradation represented by the MCM	27

Chapter 1

Introduction

Air pollution is the leading environmental health risk in many areas around the world affecting both the human population and ecology. The effects of air pollution to the general population range from chronic to less severe health impacts, and reduced growth rates of vegetation due to air pollution results in economic losses running into billions of euros per year (EEA, 2015). Moreover, air pollution has been labelled as carcinogenic by the International Agency for Research on Cancer (IARC, 2013). Due to these impacts, many governed areas introduced legislation designed to reduce concentrations of many air pollutants.

Tropospheric ozone (O_3) and particulate matter (PM) are the most problematic air pollutants over Europe with up to 98 and 93 % of Europe's urban population exposed to concentrations of ozone and PM above the WHO guidelines (EEA, 2015). Furthermore, in 2011 the EU ozone target value for human health (the EU does not currently have a limit value for ozone) was exceeded in 65 % of the EU member states and Europe's ozone target value for vegetation was exceeded in 27 % of the EU-28 agricultural areas (EEA, 2013).

Reducing atmospheric concentrations of tropospheric ozone is a complex problem as ozone is not directly emitted into the troposphere. Tropospheric ozone is produced from the reactions of nitrogen oxides ($NO_x \equiv NO + NO_2$) and volatile organic compounds (VOCs) in the presence of sunlight (Atkinson, 2000). Moreover, the photochemical nature of ozone production leads to a strong influence of meteorological variables, such as temperature and wind speed, on ozone production (Jacob and Winner, 2009).

Air quality (AQ) models are an important tool for understanding ozone pollution and for predicting future air quality. There are many AQ models available

for investigating ozone pollution with different scales and dimensions depending on the scope of the modelling experiment. Accurately representing the complexity of ozone production, such as emissions, atmospheric chemistry, meteorology and atmospheric transport, in a computationally efficient model is an ongoing challenge for the modelling community (Russell and Dennis, 2000).

Model intercomparison projects (MIPs) compare the outputs from different models, typically showing differences in tropospheric ozone due to differing representations of key processes. For example, the ACCMIP (Atmospheric Chemistry and Climate Model Intercomparison Project) showed different magnitudes of future ozone burden in the same region (Young et al., 2013). The CCMI (Chemistry Climate Model Initiative) aims to investigate differences in the representation of chemistry, emissions and transport processes between models to understand the differences between predictions from global models (Eyring et al., 2013).

Detailed process studies are key to understanding differences between model representations which could lead to differences in simulated ozone levels. This thesis determines the effects of different representations of VOC degradation chemistry, VOC emissions and the effects of temperature on ozone production. This assessment should be beneficial to the wider modelling community in understanding potential differences between model outputs and improving the current suite of models.

1.1 Ozone

Ozone is a atmospheric gas found in the stratosphere and troposphere, however its atmospheric effects are very different in these regions. About 90 % of the atmospheric ozone is present in the stratosphere with a peak mixing ratio of about 12 ppm (Seinfeld and Pandis, 2006). Stratospheric ozone absorbs the sun's ultraviolet radiation with wavelengths between 280 and 315 nm. Since excess UV radiation may cause as skin cancer, cataracts and a suppressed immune system in humans, and can also damage land and aquatic ecosystems (World Meteorological Organisation, 2011), the absorption of UV radiation by stratospheric ozone is extremely important.

In contrast, tropospheric (or surface) ozone is both a pollutant and a greenhouse gas. Increased levels of tropospheric ozone are harmful to humans, plants and other living systems. High ozone exposure may lead to pulmonary problems in humans and can decrease both crop yields and forest growth (World Meteorological Organisation, 2011).

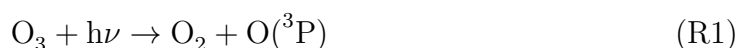
Globally, tropospheric ozone is mainly formed via photochemical production from the reactions of VOCs and NO_x , described in Sect. 1.2. Although surface ozone concentrations are also influenced by meteorology and atmospheric transport. For example, a spring-time peak in tropospheric ozone concentrations is common in the mid-latitudes of the Northern Hemisphere originally attributed to transport of ozone from the stratosphere into the troposphere via the Stratosphere-Troposphere Exchange (STE) (Monks, 2000). However, ozone transported via STE rarely influences surface ozone levels (Lelieveld and Dentener, 2000) and the spring maximum is due to the photochemical reactions occurring in the Northern Hemisphere spring after the buildup of reservoir species over winter (Penkett and Brice, 1986). These reservoir species are oxidised at a faster rate due to the increase in temperature, moisture and sunlight in spring.

Understanding the intricacies of surface ozone pollution requires a combined effort from the modelling, observational and chemical kinetic communities – called the “three-legged stool” approach by Abbatt et al. (2014). Modelling of ozone production helped in understanding the complexity of atmospheric chemistry, such as the non-linear relationship of ozone production with precursor (VOC and NO_x) emissions. Modelling studies attempt to reproduce observational trends of surface ozone and model predictions may inspire the set-up of new observational studies. Chemical kinetic studies performed by laboratories give insights to missing or incorrect representations of atmospheric chemistry which may be included in updated models.

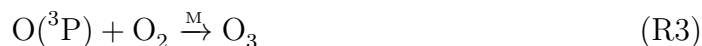
This thesis focuses on the representation of VOC degradation chemistry, VOC emissions and the ozone-temperature relationship within models and the influence on ozone production. The state of the art knowledge of ozone production chemistry is outlined in Sect. 1.2, while sources of emissions of ozone precursors are described in Sect. 1.3. Finally, the effects of meteorology, in particular temperature, on ozone production is presented in Sect. 1.4. For the rest of this thesis, ozone shall refer to tropospheric ozone.

1.2 Ozone Chemistry

Ozone absorbs UV radiation producing either ground-state atomic oxygen ($\text{O}(^3\text{P})$) or excited singlet ($\text{O}(^1\text{D})$) oxygen atoms.



Ground-state oxygen quickly reacts with oxygen to reform ozone.



Thus there is no net loss or production of ozone through (R1) and (R3). $\text{O}({}^1\text{D})$ may collide with N_2 or O_2 (represented as M in chemical reactions) stabilising to the ground-state.

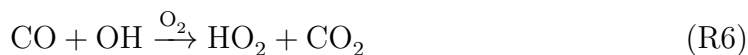


This process again leads to a null cycle with ozone destruction balanced by production. However, $\text{O}({}^1\text{D})$ can also react with water vapour producing two hydroxyl (OH) radicals.

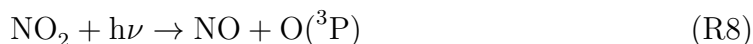


The OH radical is a highly reactive chemical species reacting with almost all trace chemical species in the troposphere but not relatively inert species such as N_2 or O_2 . OH is primarily produced via (R5) and is also catalytically produced during the degradation of VOCs. These sources of OH together lead to a relatively high daytime concentration of OH of the order of 10^6 molecules cm^{-3} . (Seinfeld and Pandis, 2006; Monks, 2005)

The initial oxidation of VOCs by OH sets off a reaction chain which may lead to net production or loss of ozone depending on the atmospheric conditions. For example, when carbon monoxide (CO) reacts with OH in the presence of oxygen, carbon dioxide and the hydroperoxy (HO_2) radical are formed. In polluted areas with high- NO_x concentrations, HO_2 readily reacts with nitrogen oxide (NO) which regenerates OH and produces nitrogen dioxide (NO_2).



Photolysis of NO_2 produces ground-state atomic oxygen producing ozone via (R3).



OH may also react with NO to produce nitrous oxide (HONO), which rapidly

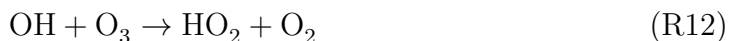
photolyses to return OH and NO.



However, termination of OH and NO₂ regeneration occurs when OH reacts with NO₂ as nitric acid (HNO₃) is formed and HNO₃ may be removed through deposition processes.



In the low-NO_x conditions away from polluted areas, OH and HO₂ are interconverted through reactions with ozone.



OH and HO₂ may also react in a termination reaction producing water vapour and oxygen.



Other termination reactions involve combination reactions of HO₂ radicals producing hydrogen peroxide (H₂O₂).



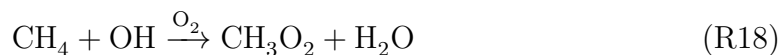
Hydrogen peroxide may be removed through deposition (Gunz and Hoffmann, 1990) but may also be a temporary sink for the odd-oxygen species OH and HO₂, represented as HO_x.



In summary, the secondary degradation of CO produces ozone in high-NO_x conditions while in low-NO_x conditions ozone is destroyed. (Seinfeld and Pandis, 2006; Monks, 2005)

The secondary degradation of higher VOCs has similar features to that of CO. Methane (CH₄) with a mixing ratio of about 1.7 ppmv is the most abundant

VOC in the troposphere. The reaction of methane with OH, in the presence of O₂, produces the methyl peroxy radical (CH₃O₂) – the simplest organic peroxy radical (RO₂).



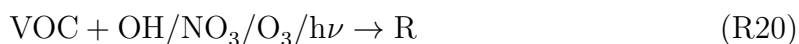
Similar to CO oxidation, the level of NO_x conditions play a crucial role in the fate of CH₃O₂ and whether ozone is produced or destroyed, this is depicted graphically in Fig. 1.1.



Many thousands of VOCs are emitted into the atmosphere from anthropogenic and biogenic sources, discussed further in Sect. 1.3. Despite the vast array of VOCs, there are many common features between the degradation pathways. Figure 1.2 represents a general and simplified reaction scheme for VOCs in the troposphere.

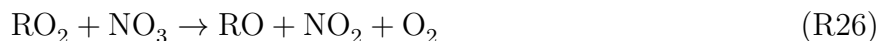
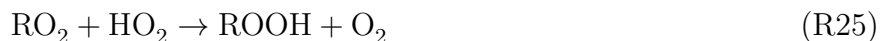
The primary oxidation of a VOC is typically through reaction with the hydroxyl (OH) radical.

The reaction of a VOC with OH forms an alkyl or substituted alkyl radical (R) which in the presence of O₂ produces alkyl peroxy radicals (RO₂). Unsaturated VOCs, such as alkenes, may also react with ozone while photolysis is a primary degradation pathways for carbonyl species. During the night-time, reaction with the nitrate (NO₃) radical is of importance. These initial reaction pathways all lead to the formation of RO₂ radicals.



RO₂ radicals can subsequently react with NO, NO₂, hydroperoxy (HO₂) radicals, NO₃ radicals - mainly during night-time - and with other alkyl peroxy radicals (Atkinson, 2000). The competition between these reactions, especially those pathways involving NO_x ((R22), (R23) and (R24)), determines whether net

production or loss of ozone occurs.



All reactions pathways of RO_2 that produce NO_2 can result in O_3 formation due to (R8) and (R3). Reaction with the HO_2 radical forms a hydroperoxide (ROOH) which then photolyses producing an alkoxy (RO) radical and recycling an OH radical. The carbonyl and alcohol products resulting from reaction with other RO_2 radicals will follow a similar sequence of reactions and hence can also produce further O_3 . Thus the secondary degradation products of a VOC may also lead to further production of ozone.

Reaction of RO_2 with NO_2 leads to the formation of peroxy nitrates (RO_2NO_2) which are a temporary reservoir for RO_2 and NO_x . When temperatures are low, the thermal decomposition of RO_2NO_2 to recycle RO_2 and NO_x happens at a slower rate than at higher temperatures. Hence, at lower temperatures RO_2NO_2 may build up and be transported away from their region of formation and re-release RO_2 and NO_2 downwind fuelling ozone production away from large sources of NO_x . This is one example of the dependence of ozone production on meteorological variables, a broader overview is given in Sect. 1.4.

The secondary degradation of the RO radical formed from many of the RO_2 reactions proceeds through either decomposition, isomerisation or reaction with O_2 . The products that result from the reaction pathways depend on the parent VOC and this also determines the number of NO -to- NO_2 conversions, eventually leading to O_3 formation.

The final degradation products of VOCs are carbon dioxide (CO_2) and water vapour. The path that each VOC takes to reach its final products is dependent on the type of VOC, the radical concentration, the NO_x concentration and other factors such as time of day and year. The detailed atmospheric chemistry of most VOCs is well-understood however for more complex VOCs the complete set of reaction pathways of all the secondary degradation products there are a great number of

uncertainties. These uncertainties may be related to kinetic data, photolysis rates, reaction branching ratios and in most cases the reaction products. Any uncertainties in reaction pathways and products of VOCs also leads to uncertainties in estimating the amount of ozone produced during the degradation of a particular VOC (Atkinson, 2000).

1.2.1 VOC and NO_x Chemistry

One of the most important features of ozone production, briefly hinted at previously, is the dependence of ozone levels on both VOC and NO_x. Figure 1.3, from Jenkin and Clemitshaw (2000), depicts the non-linear relationship between O₃ mixing ratios as a function of VOC and NO_x mixing ratios. This relationship can be divided into distinct regimes of ozone production: *NO_x-sensitive* (or *NO_x-limited*), *NO_x-saturated* (or *VOC-sensitive*) and *VOC-and-NO_x-sensitive* regimes.

The cause of the non-linear relationship is the pathways available to RO₂. In the NO_x-sensitive regime, the concentration of NO_x is low compared to that of radicals hence radicals are more likely to react with other radicals. The most common reactions are bimolecular destruction (R14), which removes radicals, or combination of radicals (R25) into reservoir species that can re-release radicals.

Reactions between radicals do not directly lead to ozone production as little NO is converted to NO₂. Thus increasing NO_x would increase the number of NO to NO₂ reactions by peroxy radicals leading to ozone production. However, increasing VOC levels would not increase O₃ production as increases the likelihood of radical destruction or combination reactions.

The NO_x-saturated regime corresponds to high NO_x concentrations where radicals will tend to react with NO_x. Increased NO_x levels will not increase O₃ production due to an increase in nitric acid (HNO₃) formation (R11). Nitric acid is a sink for both OH and NO_x removing OH which would otherwise react with emitted VOC to fuel further radical production.

The VOC-and-NO_x-sensitive regime is characterised by O₃ production being sensitive to both VOC and NO_x levels. Moreover, it is in this atmospheric regime that the maximum amount of ozone is produced and corresponds to the contour ridges in Fig. 1.3. The non-linear relationship can be thought of as a titration process between the amount of radicals and the NO_x present in the atmosphere with the VOC-and-NO_x-sensitive regime being the turning point (Kleinman, 1991, 1994).

This non-linear nature of the troposphere to ozone production makes controlling ozone levels particularly difficult. The difficulty is exacerbated by the fact that regions can alternate between these regimes depending on the season, time of day etc. Moreover, fresh emissions tend to occur in the NO_x -saturated regime and through transport, the emissions are advected to VOC-and NO_x -sensitive and even NO_x -sensitive regions.

1.2.2 Representing Atmospheric Chemistry in Models

Representing this complex chemistry for each emitted VOC in a chemical transport model (CTM) is unrealistic. Even if all the secondary degradation pathways and products were known for every VOC, a CTM would not be able to efficiently numerically solve the resulting differential equations. Hence, CTMs use descriptions of atmospheric chemistry that lead to more computationally efficient models.

Not all representations of atmospheric chemistry used in a *chemical mechanism* are prepared in the same way. For a start, models that also numerically compute meteorology fields require very computationally efficient chemical mechanisms including around 150 unique species while simpler box models can use chemical mechanisms having many thousands of species. The simplification techniques used to represent the multitude of VOC and their degradation may lead to discrepancies in the estimations of ozone production. We compare the ozone production from many reduced chemical mechanisms to a highly detailed chemical mechanism in Sect. 3.1 and the research questions addressed in this study are framed in Sect. 1.5.

use
Stockwell:2012
review

1.3 Emissions of Ozone Precursors

1.3.1 NO_x

Emissions of NO_x are mainly through anthropogenic activity. In the year 2000, almost 52 Tg N were emitted with 65 % through the many forms of fossil fuel combustion (Seinfeld and Pandis, 2006). Examples of fossil fuel combustion that releases NO_x are transportation using diesel or petrol vehicles, industrial activities and domestic heating (von Schneidemesser et al., 2015).

Up to 95 % of NO_x emissions from combustion are emitted as NO, which

then is oxidised to form NO_2 through (R19) and (R23). However, due to the increase in diesel vehicles and the implementation of diesel filters the fraction of emitted NO_2 has increased. Grice et al. (2009) showed that over Europe, emissions of NO_2 from diesel vehicles has increased from 8.6 % in 2000 to 12.4 % in 2004.

Despite the overwhelming majority of NO_x emissions coming from human activities, there are many important natural sources of NO_x . Lightning and soils are also important sources of NO_x , each source contributed about 10 % to global NO_x emissions in 2000 (Seinfeld and Pandis, 2006).

1.3.2 VOCs

Carbon Monoxide

Carbon monoxide, CO, is emitted directly into the troposphere through combustion and industrial processes. Another equally-important source of CO, is its chemical formation during the degradation of VOCs. Hauglustaine et al. (1998) estimated that globally 881 Tg yr^{-1} of CO was produced from chemical oxidation of VOC while 1219 Tg yr^{-1} of CO was directly emitted.

Oxidation of CO, through reaction with OH, is its major atmospheric sink and can lead to ozone production. When the hydroperoxy radical (HO_2) reacts with NO, NO_2 is formed which may produce ozone and OH is again recycled and available to further oxidise other chemical species.

The maximum possible yield of ozone from the degradation of a single molecule of CO occurs when each peroxy radical converts NO to NO_2 . In this case, a maximum of one molecule of ozone can be produced per molecule of CO oxidised. In reality, this is never achieved as other reactions with the peroxy radicals occur however this is a very informative measure of the *ozone production potential* of a species.

Methane

Emissions of methane are between 500 and $600 \text{ Tg CH}_4 \text{ yr}^{-1}$ with about 60 % of the emissions from anthropogenic sources. The main anthropogenic sources of CH_4 are agriculture, fossil fuels and biomass burning with agriculture contributing 60 % of the anthropogenically emitted methane. Emissions from wetlands are the

main natural source of methane emissions (Kirschke et al., 2013).

Reaction with OH is the main sink of methane and this reaction is important for the concentration of OH in the troposphere. With increased methane emissions, the concentration of OH will decrease via (R18) which would lead to a build of methane and other VOCs in the troposphere (Holmes et al., 2013).

The secondary degradation of methane produces the methylperoxy radical CH_3O_2 as well as HO_2 as well as CO. Assuming that every peroxy radical converts NO to NO_2 then methane degradation can produce a maximum five molecules of O_3 per molecule of CH_4 oxidised. Methane (CH_4) has a lifetime of about 9 years, significantly longer than all other VOCs. Thus, methane influences ozone production on the global rather than the regional scale.

Non-Methane VOCs

A wide variety of non-methane VOC (NMVOC) are emitted from anthropogenic activities directly into the troposphere. Solvent use, industry, fossil fuel burning and transportation are all major activities emitted NMVOCs of varying functional groups and carbon numbers. The maximum number of molecules of O_3 produced per degradation of an emitted NMVOC depends on the number of NO to NO_2 conversions by the peroxy radicals formed during the degradation of the NMVOC. This is highly dependent on the type of NMVOC and the number of carbons in the NMVOC.

Many NMVOCs emitted from anthropogenic sources are also hazardous to human health in their own right. For example, benzene and formaldehyde are suspected carcinogens (Laurent and Hauschild, 2014). It is also worthwhile to note that the NMVOC thought to be the most hazardous to human health do not correspond to NMVOC that have a high ozone production potential.

Globally, Lamarque et al. (2010) estimated that 130 Tg NMVOC were emitted from anthropogenic sources in the year 2000. This amount is dwarfed by the total emissions from biogenic sources – 1000 Tg NMVOC yr^{-1} , almost eight times the amount of NMVOC emitted from anthropogenic sources (Guenther et al., 2012).

Of the NMVOC emitted from vegetation, isoprene (C_5H_8) dominates at the global scale however emissions of monoterpenes and sesquiterpenes are also significant. There is typically overlap in the NMVOC species emitted from biogenic and anthropogenic sources. For example, isoprene has also been measured in the

urban areas of London and Paris away from direct emission sources and since isoprene is a very reactive NMVOC it is unlikely to be transported from outside the area, there appears to be anthropogenic sources of isoprene (von Schneidemesser et al., 2011). Also many small NMVOC that are typically emitted from anthropogenic sources, such as methanol and acetaldehyde, are also emitted from vegetation (Guenther et al., 2012).

The NMVOC species emitted vary between types of vegetation – some trees emit large amounts of isoprene while others do not. Also, the quantity of NMVOC emissions from vegetation depends on atmospheric (such as, temperature and radiation) and biological variables (such as, leaf age and leaf area index). Thus only regulation of NMVOC from anthropogenic sources is possible and drastic reductions in anthropogenic NO_x are required to minimise the burden of the population to ozone pollution. Areas dominated by biogenic NMVOC emissions and away from large NO_x sources (NO_x -sensitive regime) could lead net loss of ozone through direct reactions of ozone with many biogenic NMVOC and the net loss of radicals (discussed in Sect. 1.2.1).

1.3.3 Representing VOC Emissions in Models

Representing the multitude of emitted VOCs, from either anthropogenic or biogenic sources is one of the major challenges of the modelling community. Models use emission inventories that specify the type and quantity of VOCs emitted over a region or even the whole globe. However, as hinted at, this is no easy task and emission inventories are one of the major sources of uncertainty of the model input (Russell and Dennis, 2000).

Emission inventories typically specify emissions for NO_x , CO, CH_4 , NMVOC as well as non-gas-phase emissions such as particulate matter. Emissions are assigned to source sectors, called SNAP (Standardised Nomenclature for Air Pollutants) sectors, such as those listed in Table 1.1. The rest of this section shall discuss specifications of NMVOC emissions from emission inventories.

Emissions of both NO_x and VOCs are not constant over the year, month or time of day. In many regions, a noticeable reduction in NO_x emissions, due to reduced road transport, is noted during the weekend – called the “weekend-effect”. The weekend-effect has implications on the ozone production during the weekend. For example, ozone production is NO_x -saturated during weekdays in San Joaquin Valley, California. The reduction of NO_x emissions during the weekend moves ozone

Table 1.1: SNAP sectors for anthropogenic emissions listed in the TNO_MACCIII inventory (Kuenen et al., 2014).

SNAP Sector	Description
1	Public Power
2	Residential Combustion
34	Industry
5	Fossil Fuel
6	Solvent Use
71	Road Transport: Gasoline
72	Road Transport: Diesel
73	Road Transport: Others
74	Road Transport: Evaporation
75	Road Transport: Wear
8	Non-road Transport
9	Waste
10	Agriculture

production to the VOC-and-NO_x sensitive regime, hence higher ozone levels are measured during the weekend (Pusede et al., 2014).

Anthropogenic NMVOC emissions from the different SNAP sectors also have a temporal distribution. Many SNAP sectors, such as industry and solvent use, have a reduction in emissions on weekends. Transport emissions tend to peak during the morning and evening rush hours and emissions due to solvent have a strong diurnal cycle. Residential combustion tends to be highest during the winter months and lowest during the summer (Denier van der Gon et al., 2011).

Emission factors are assigned to the emissions from SNAP categories to represent the temporal profiles within a model. Biogenic VOC emissions are typically estimated using an algorithm including variables on which BVOC emissions are dependent. MEGAN2.1 (Guenther et al., 2012) is commonly used by the modelling community to represent emissions from nature. The MEGAN2.1 model utilised variables such as temperature and radiation levels which are calculated during model simulations and then fed into the MEGAN2.1 model to estimate BVOC emissions.

One issue for the modelling community with using emission inventories for specifying NMVOC emissions is translating the listed emissions into the chemical species used by the chemical mechanism. Emission inventories are not normally immediately available for use with a chemical mechanism which can lead to different modelling groups allocating the emission inventory input differently for the same chemical mechanism (Carter, 2015). Chemical mechanisms used in global and regional models cannot represent each NMVOC individually for reasons of computational

Table 1.2: Influence of meteorological variables on ozone production, taken from Jacob and Winner (2009).

Meteorological Variable	Influence on Ozone
Temperature	Consistently positive
Regional Stagnation	Consistently positive
Wind Speed	Generally negative
Mixing Depth	Weak or variable
Humidity	Weak or variable
Cloud Cover	Generally negative
Precipitation	Weak or variable

efficiency thus many NMVOCs must be represented by the particular lumped (or aggregated) species of the chemical mechanism. This translation into lumped species differs between chemical mechanisms (Sect. 1.2.2). The effect that lumping emissions of NMVOC into different chemical mechanism has on simulated ozone production is explored in this work in Sect. 3.2.

1.4 Effects of Meteorology on Ozone Production

As the chemical processes of ozone production are photochemical in nature, meteorology has a significant influence on the amount of ozone produced. The influence of meteorology on ozone production is particularly important for predicting air quality in a world under the effects of climate change and the effects changed weather systems would have. Climate change is predicted to influence many meteorological variables that impact ozone production, Table 1.2, taken from Jacob and Winner (2009), details the effects specific meteorological variables have on ozone production.

Temperature

Temperature is positively correlated with ozone in many areas. Otero et al. (2016) showed that temperature was the main driver of summertime ozone values over many areas of central Europe while Camalier et al. (2007) correlated ozone with temperature over the Eastern US. Interestingly only ozone pollution (higher values of ozone) and not background ozone, the ozone levels without the influence of anthropogenic emissions. is correlated with temperature (Sillman and Samson, 1995).

Temperature positively influences ozone levels directly in two ways:

increasing the emissions of VOCs from vegetation and speeding up the rates of chemical reactions. Pusede et al. (2015) reviewed the chemical processes that exhibit temperature dependency and the relation of temperature on ozone production. The production of radicals (OH , HO_2 , RO_2) and temperature-dependence of organic reactivity strongly influence the production of ozone. The shorter lifetime of peroxy nitrates at higher temperatures, increased radical production during VOC degradation, changes in emissions of both VOC and NO_x and formation of alkyl nitrates (R23) all exhibit temperature dependent influences on ozone production.

Despite many studies from an observational and regional modelling perspective correlating temperature with ozone production, there has been a lack of detailed process studies separating the direct effects of temperature on ozone. Moreover, there are no attempts to tease the relative importance of the chemical processes listed in Pusede et al. (2015) on ozone production. The final part of this study addresses the whether higher emissions or faster chemistry is more important for ozone production and also which chemical processes are the most important for ozone production. The results of this study are presented in Sect. 3.3.

Humidity

Humidity levels influences ozone production both positively and negatively. When O^1D , coming from ozone photolysis (R2), reacts with water vapour (R5), the production of OH radicals leads to ozone loss. However, the initiation of VOC degradation through reaction with OH can lead to ozone production as described in Sect. 1.2. These competing effects of water vapour on ozone production leads to a weak correlation of ozone production with water vapour (Jacob and Winner, 2009).

Wind Speed and Stagnation

High wind speeds transport ozone precursors away from their sources leading to a generally negative effect on ozone pollution over a region. Doherty et al. (2013) projected using a multi-model study that while climate change is expected to change large-scale atmospheric transport, model projections show that these have little influence on the spatial patterns of mean concentrations of ozone.

When low wind speeds are present over polluted urban areas stagnant conditions arise and these atmospheric conditions are highly correlated with increased ozone production over urban areas (Jacob and Winner, 2009). Typically stagnant

conditions are also related to periods of high temperatures which may further fuel ozone production. During periods of stagnant conditions, the ozone produced from the previous day (the ozone-lag) is not transported downwind, add the ozone production from emissions of ozone precursors and this leads to high ozone episodes (Jacob and Winner, 2009).

Mixing Height

The effects of increased mixing heights of the planetary boundary layer (PBL) with the free troposphere are not so straightforward. Dawson et al. (2007) found that over the Eastern U.S., regions with low ozone are positively correlated with mixing height whereas regions with high ozone levels are negatively affected. This spatial effect of mixing height on ozone production comes from whether the free troposphere ozone levels are higher or lower than the ozone levels within the PBL (Jacob and Winner, 2009). The study of Dawson et al. (2009) showed that the predicted lower PBL heights coupled with stagnant conditions led to increased levels of ozone.

1.5 Research Questions

The overarching research question of this thesis is to determine detailed chemical processes affecting tropospheric ozone production. This broad question is further focused on detailed modelling studies that bring out which chemical processes have the largest impact on tropospheric ozone production. The focus of the study is further narrowed to look at the important chemical processes affecting ozone production under three different conditions that influence .

Firstly, AQ models have a choice in the representation of the chemistry, these chemical mechanisms are produced using different approaches which may impact on ozone production. Furthermore, the scope of a modelling study (point, regional or global) may limit the choice of chemical mechanism to an extremely simplified version of the complex atmospheric chemistry detailed in Sect. 1.2. Thus leading to the first research questions:

- How do the simplification techniques used in different chemical mechanisms affect ozone production?
- Does the choice of chemical mechanism impact predicted ozone production?

Secondly, the model inputs are critical for modelling studies and the specified inputs of NMVOC emissions are known to be a large source of uncertainty. Emission inventories specify the NMVOCs emitted from different anthropogenic activities. Different emission inventories are available to the modelling community and these may vary the speciations of different NMVOCs for the different sectors of anthropogenic activity. We narrowed the focus to the solvent use sector, the sector with the largest percentage emissions, and used these different speciations to address the following questions:

- What is the influence on predicted ozone production when using different speciations of emitted NMVOCs?
- How does this influence change when using different chemical mechanisms?

Finally, meteorology influences the amount of ozone production with temperature being listed as the meteorological variable with the strongest positive correlation with ozone. Temperature influences the amount of emissions from biogenic sources and also influences the reaction rates of chemical reactions. These effects have been noted in many modelling and observational studies but not under varying NO_x conditions that would lead to the different NO_x regimes of the atmosphere.

- Are temperature dependent emissions or temperature dependent chemical processes more important for ozone production with increasing temperature?
- How is temperature dependent ozone production treated in different NO_x regimes within a box model?

Chapter 2 details the methodology used to address these questions in greater detail. The results from the separate studies and relevant publications are found in Chap. 3. A broader discussion of the answers to the above research questions and their applications to the AQ modelling community are discussed in Chap. 4.

Figure 1.1: Methane degradation pathways in low- NO_x and high- NO_x conditions. Taken from Monks (2005).

Figure 1.2: Schematic diagram outlining general pathways of the secondary degradation of an emitted VOC.

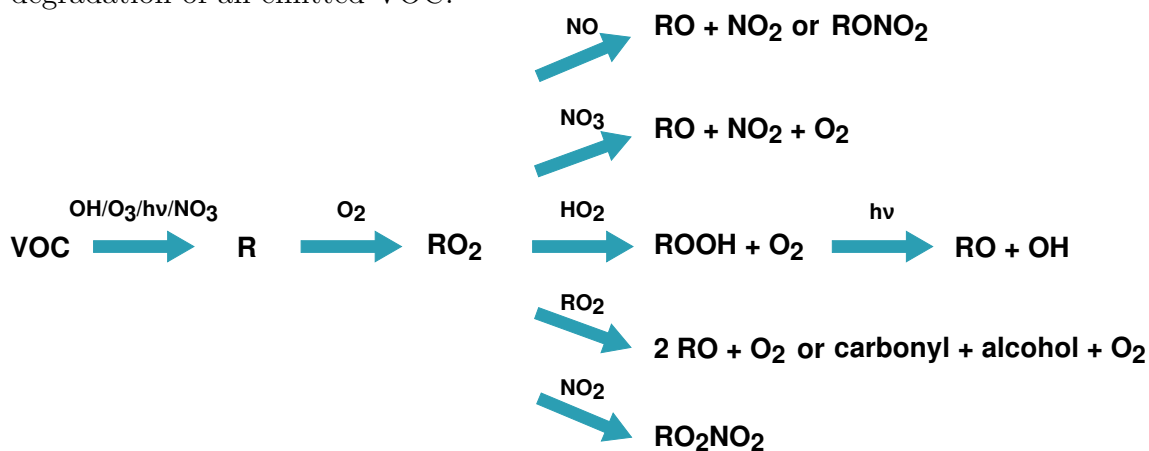
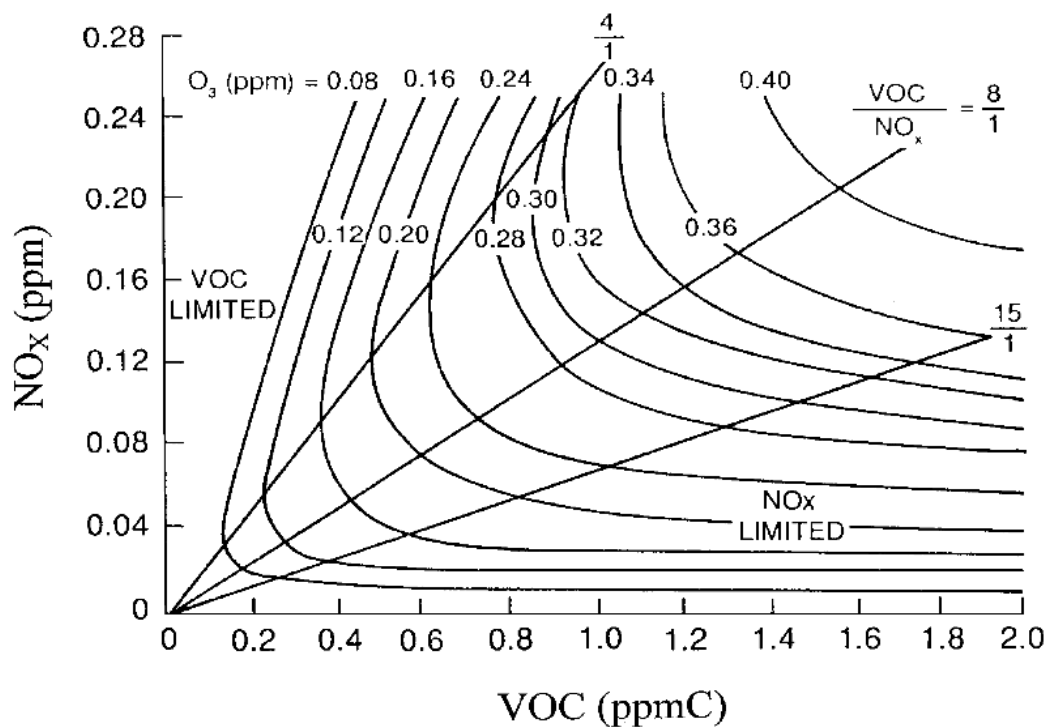


Figure 1.3: Ozone isopleth plots for various initial mixing ratios of NO_x and a VOCs. taken from Jenkin and Clemmitshaw (2000).



Chapter 2

Methodology

This chapter describes the methods and materials used throughout the study to address the research questions of the study (Section). Details of the modelling set-up, including initial and boundary conditions are included in this chapter.

add section
number

2.1 Air Quality Modelling

Photochemical models are used to predict future air quality scenarios. A large array of these models are used depending on the study focus, for example, global photochemical models can predict air quality on a global scale and include the relevant chemical and dynamical processes whereas an urban model focuses on a particular urban area and includes the relevant processes (such as topography, local emission source) to the area being studied. Despite differing scopes between models, there are a number of common inputs including emissions of chemical species into the model, transport of the species, atmospheric physical and chemical transformation and numerical solutions to the applicable differential equations.

Models are usually defined as either Eulerian or Lagrangian, with Eulerian models constituting most of the models used in the air quality modelling community (Russell and Dennis, 2000). Eulerian models describe the atmosphere by fixed computational cells where species enter in and out of the cell walls and the concentrations of the species within each cell are calculated as a function of time. Whilst Lagrangian models simulate changes of selected air parcels during advection through the atmosphere, hence there is no mass exchange between the surroundings and the air parcel (besides the emissions) and the model calculates concentrations at

different locations at different times (Seinfeld and Pandis, 2006).

Photochemical models also have different dimensions, ranging from zero-dimensional (box model) to three-dimensional models where the simplicity and computing power increase with the dimension of the model. 3-D models calculate atmospheric concentrations as a function of latitude, longitude, altitude and time. While 2-D models assume that concentration is a function of latitude and altitude (but not longitude) and time. Column models (or 1-D models) use concentrations that are a function of time and height. Box models are the simplest type of a model and have uniform atmospheric concentrations that are only a function of time (Seinfeld and Pandis, 2006).

Box models lack physical realism and essentially focus on processes relevant to a point in the atmosphere. Despite the lack of realism, box models are extremely useful for studying the detailed processes that influence air quality. Examples of modelling studies that have used box models include Qi et al. (2007), Li et al. (2014) and Nölscher et al. (2014).

All photochemical models numerically solve the chemical species conservation equation which describes the processes affecting the concentration of the different species:

$$\frac{\partial c_i}{\partial t} + \nabla \cdot \bar{U}c_i = \nabla \rho D \nabla (c_i/\rho) + R_i(c_1, c_2, \dots, c_n, T, t) + S_i(\bar{x}, t), \quad i = 1, 2, \dots, n. \quad (2.1)$$

In Eq. (2.1), c_i is the concentration (in mass or volume) of species i , \bar{U} is the wind velocity vector, D_i is the molecular diffusivity of species i , R_i is the rate of concentration change of species i through chemical reactions, $S_i(\bar{x}, t)$ is the source or sink of i at location \bar{x} , ρ is the air density and n is the number of predicted species. R may also be a function of meteorological parameters such as temperature T and S includes emission and deposition processes affecting i (Russell and Dennis, 2000).

re-word this
as too similar
to citation

The dimension and type of the model determine the set of differential equations that will be solved at each time step of the model run. Numerical methods to determine the concentration of species i in Eq. (2.1) vary between models, examples include Runge-Kutta (Sandu et al., 1997b), Finite Element (Russell and Dennis, 2000) or Rosenbrock methods (Sandu et al., 1997a).

Initial and boundary conditions are required to numerically solve the system of differential equations. Boundary conditions are typically the most difficult input to set accurately as this requires knowledge of the investigated species concentrations

and transport at the boundary edges (if applicable) of the model grid. Setting the initial conditions involves fixing the starting concentrations of the species being studied, these conditions are dependent on the area being studied and whether it is an urban or rural area, amongst other considerations.

2.1.1 Model Description and Setup

In order to assess the detailed processes producing tropospheric ozone within general air quality modelling, we used a box model to focus on the gas-phase chemistry affecting tropospheric ozone. All simulations in this study were performed using the MECCA (Module Efficiently Calculating the Chemistry of the Atmosphere) box model developed by Sander et al. (2005) that was adapted to include MCM v3.1 chemistry as described in Butler et al. (2011). The MECCA box model has been used for numerous detailed process studies of atmospheric gas-phase chemistry including Kubistin et al. (2010), Xie et al. (2008) and Lourens et al. (2016).

MECCA is written using the FORTRAN programming language and runs on UNIX/Linux platforms. The setup of MECCA that we used uses the KPP (Kinetic Pre-Processor) (Damian et al., 2002) to efficiently setup up the system of differential equations (Eq. (2.1)). KPP processes the specified chemistry scheme in the chemical mechanism and generates Fortran code that is then compiled by MECCA. KPP also has numerous choices for the numerical solver used to numerically determine the concentrations of all the species described by the chemistry. We have used a Rosenbrock solver (the `ros3` option) throughout the study.

Aside from the chemistry, MECCA also calculates physical parameters at every time step of the simulations. In our simulations, the pressure, temperature, relative humidity and boundary layer height are held constant at the set values of Table 2.1. The specific changes to these parameters that were systematically varied to answer the research question related to are detailed in the relevant publication (Chapter).

add section

TBC about this

Photolysis rates in this study are calculated by using a paramaterisation that calculates the photolysis rate as a function of the solar zenith angle. This paramaterisation requires the degree of latitude for the study to be a defined variable in MECCA, we have chosen the 34° N latitude which is roughly that of the city of Los Angeles. The simulations start at the spring equinox (27th March) at 6am and allowed to run for seven diurnal cycles.

Table 2.1: General settings used for MECCA box model in this study

Model Parameter	Setting
Pressure	1013 hPa
Temperature	293 K
Relative Humidity	81 %
Boundary Layer Height	1000 m
Latitude	34° N
Starting Date and Time	27th March 06:00
Model Time Step	20 mins
Model Run Time	7 days

In our setup of MECCA, all fluxes into and out of the box are handled by KPP. The chemical mechanism file, processed by KPP, includes specific pseudo-unimolecular reactions specifying the emissions and dry deposition of chemical species along with the relevant rate. The chemical species that are emitted into the model and the emission rates are read into the model using a namelist file. Namelist files are also used to specify the initial conditions of chemical species and the mixing ratios of those chemical species that are fixed throughout the model. In all simulations, methane (CH_4) was fixed to 1.75 ppmv while carbon monoxide (CO) and O_3 are initialised at 200 ppbv and 40 ppbv and then allowed to evolve freely.

2.2 Chemical Mechanisms

The atmospheric chemistry in AQ models is described by the chemical mechanism used by the AQ model. The chemical mechanism includes rate coefficients, reaction pathways with the corresponding branching ratios, photolysis rates and reaction products which are required to solve the concentrations of each chemical species within the system using Equation (2.1).

Different modelling scopes and models determine the level of chemical detail of the chemical mechanism used by the AQ model, thus many different chemical mechanisms have been developed by the AQ modelling community. The level of detail included in the chemical mechanism determines the amount of computing resources required for the model simulations, hence the chemical mechanism in a 3-D model will typically be less detailed than the chemical mechanism used by a box model.

Chemical mechanisms range from highly-detailed (explicit) chemical mechanisms to the less-detailed lumped-structure and lumped-molecule chemical

Table 2.2: Chemical mechanisms used in the study.

Chemical Mechanism	Lumping Type	Reference
MCM v3.1 and v3.2	No lumping	Jenkin et al. (1997), Jenkin et al. (2003) Saunders et al. (2003), Bloss et al. (2005) Rickard et al. (2015)
CRIV2	Lumped intermediates	Jenkin et al. (2008)
MOZART-4	Lumped molecule	Emmons et al. (2010)
RADM2	Lumped molecule	Stockwell et al. (1990)
RACM	Lumped molecule	Stockwell et al. (1997)
RACM2	Lumped molecule	Goliff et al. (2013)
CBM-IV	Lumped structure	Gery et al. (1989)
CB05	Lumped structure	Yarwood et al. (2005)

mechanisms. The self-generating chemical mechanism of Aumont et al. (2005) is an example of an explicit chemical mechanism and includes many thousands of reactions outlining the degradation chemistry of VOCs, outlining even the reactions generating degradation products of minor importance in the atmosphere. Near-explicit chemical mechanisms, such as the Master Chemical Mechanism (MCM) of Jenkin et al. (1997), Jenkin et al. (2003), Saunders et al. (2003), are less-detailed than self-generating mechanisms but still contain many thousands of reactions and as such are mainly used in box models. The MCM representation of VOC degradation chemistry is discussed in more detail in Sect. 2.2.1.

Many other chemical mechanisms have been developed to describe atmospheric chemistry using less-detailed descriptions as those used by explicit and near-explicit chemical mechanisms so that these chemical mechanisms are computationally efficient for use within 3-D models. These reduced chemical mechanisms have been developed using a number of different techniques which ultimately lead to aggregating (lumping) VOC into mechanism species, these mechanism species are then degraded in such a way that the chemical production of ozone is similar to that from observational records. The first part of this study compares the maximal ozone produced from a number of reduced chemical mechanisms, listed in Table 2.2, a description of the different reduction techniques used by the reduced mechanisms is found in Sect. 2.2.2, Sect. 2.2.3 and Sect. 2.2.4. The main results from the chemical mechanism comparison study are presented in Sect. 3.1.

2.2.1 Near-Explicit Chemical Mechanisms

The Master Chemical Mechanism (MCM v3) is a near-explicit mechanism describing the chemical degradation of 107 non-aromatic VOCs in (Saunders et al.,

2003) and 18 aromatic VOCs in (Jenkin et al., 2003). The MCM v3.2 was used as the reference mechanism for this study as it was the most recent version of the MCM at the time of the first experiments related to the chemical mechanism study; the MCM v3.2 was obtained from the world wide web (<http://mcm.leeds.ac.uk/MCMv3.2/>). In total, the MCM v3.2 has 12,691 reactions including 4351 organic compounds and 46 inorganic compounds. The primary VOCs represented by the MCM v3.2 were determined by which VOC have the most emissions (by mass) as listed by the UK National Atmospheric Emissions Inventory and makes up about 70% of the mass emissions of unique species achieved.

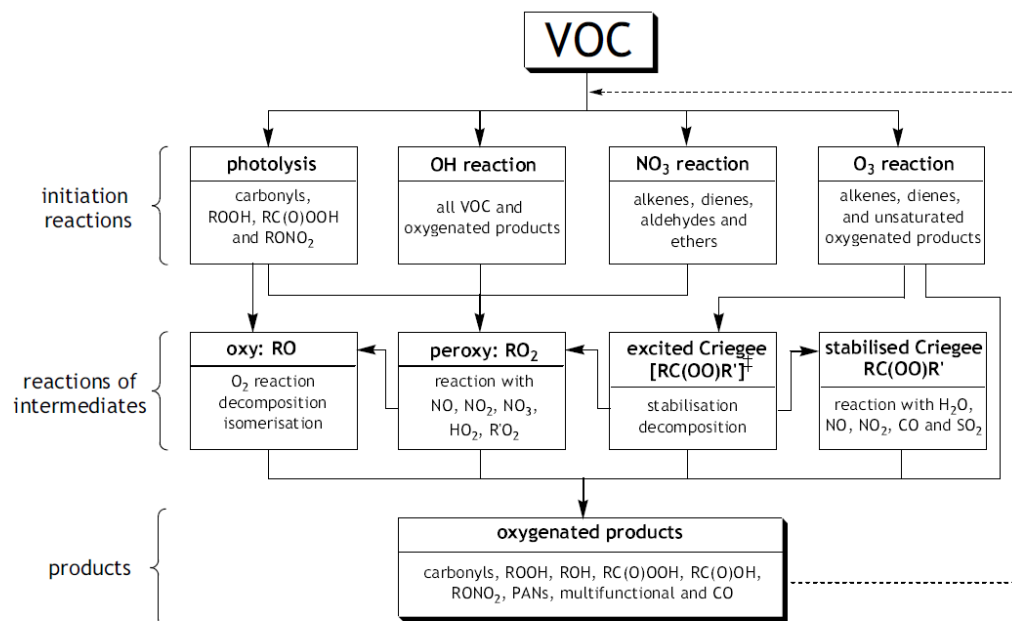
Each primary VOC and each degradation product, is individually degraded until it is broken down to CO_2 , H_2O , CO or an organic product (or radical) already represented by the MCM (Jenkin et al., 1997). Jenkin et al. (1997) outlines the main assumptions used when developing the MCM in order to reduce the number of chemical species and reactions, these include:

1. limiting the number of product channels resulting from reaction with the OH radical by disregarding pathways of low probability,
2. representing permutation (self and cross) reactions of organic peroxy radicals by a single parameterised reaction, and
3. simplifying the degradation chemistry, especially for those products deemed to be of minor importance.

Figure 2.1 shows the reaction pathways represented in the MCM of the primary VOC. The main reaction pathway for VOC degradation is by reaction with the OH radical, while ozonolysis is only important for alkenes, dienes, monoterpenes, some aromatic VOCs and some unsaturated oxygenated products. Reaction with the NO_3 radical is mainly important during the night-time and only included for alkenes, dienes, aromatics, aldehydes and ethers. Rate constants and branching ratios of the reactions represented in the MCM v3.2 are those recommended by IUPAC. If no data was available then they are estimated using structure activity representation (SAR) or group reactivity (GR) methods.

The degradation products of the primary VOCs are also treated in detail, with the first generation products also degraded further as part of the MCM. Those degradation products having significant tropospheric concentrations are treated in detail by the MCM otherwise the further degradation is limited to reaction with the OH radical. Those products deemed of minor importance are also greatly simplified whilst retaining product lifetimes and maintaining the carbon and nitrogen balance.

Figure 2.1: Flowchart of the major reactions of primary VOCs, intermediates and products considered in the MCM. Taken from Fig. 1 in Saunders et al. (2003)



2.2.2 Lumped Intermediate Chemical Mechanisms

Chemical mechanisms which aggregate (lump) the degradation products rather than primary VOC are called lumped intermediate chemical mechanisms. The Common Representative Intermediates (CRI) chemical mechanism (Jenkin et al., 2008) is an example of a lumped intermediate mechanism.

The CRI is a reduced version of the MCM that can be used in 3-D AQ models. Reducing the complexity of the MCM was achieved by representing many degradation products (intermediates) in the CRI by a single mechanism species, rather than lumping primary VOC into a mechanism species. These intermediates are designed to produce the same amount of ozone as when using the MCM. The CRI v2 was used in this study and the intermediates in this version of the CRI mirror the ozone production from the MCM v3.1.

The CRI v2 is available online (<http://mcm.leeds.ac.uk/CRI>) in a full version and further reduced variants that include even further reductions to the chemistry represented in MCM v3.1 by also lumping VOCs into lumped mechanism species. Jenkin et al. (2008) describes the main assumptions made in order to condense the organic chemistry of the MCM v3.1 to the lumped intermediate chemistry of the CRI v2, while Watson et al. (2008) describes the further reductions made to the

CRI v2 to produce the five lumped emission variants. The most reduced version of the CRI v2 has also been implemented into the widely used 3-D regional model WRF-CHEM as described in Archer-Nicholls et al. (2014).

The approach used to develop the CRI involves determining the potential number of NO-to-NO₂ conversions by the peroxy radicals formed during the degradation of a VOC, this is called the CRI-index. The CRI-index is thus the potential number of ozone molecules produced during the degradation of a VOC as the number of potential NO-to-NO₂ conversions by peroxy radicals is directly related to the potential number of O₃ molecules (Sect.). A single “common representative” is created to represent a part of the secondary degradation of a large number of species based on the CRI-index that was calculated based on the description of the degradation of the VOC in the MCM (Jenkin et al., 2008). This approach greatly reducing the number of species and reactions in the CRI compared to the near-explicit representation of the MCM.

The mechanism intermediate species are further optimised by performing multi-day model runs comparing the ozone produced from a single VOC in the CRI v2 to that in MCM v3.1. These model runs were performed for each of the primary VOC represented in the MCM v3.1 and CRI v2, starting with the smallest VOC of a particular functional group and only moving to the next largest VOC once the ozone production was optimised to that of the MCM v3.1. The primary criterion in these tests was ozone formation, the ozone formation of the mechanism intermediate species was optimised to that in the MCM v3.1 using a non-linear least squares fitting and the agreement was improved by varying the OH-reactivity and photolysis rate of the intermediate species. The individual testing of the intermediates for each VOC also showed that some intermediates did not directly follow the CRI-index rule and in-place adjustments were required to retain the ozone formation in the MCM v3.1. This approach was used for OH, O₃ and NO₃ initiated degradation (Jenkin et al., 2008).

Despite the large reductions to the MCM v3.1 chemistry to produce the CRI v2 described in Jenkin et al. (2008), the number of reactions are still too many to guarantee computational efficiency for use in 3-D models. Further reductions were made by lumping VOC emissions to produce five further reduced variants of the CRI v2; the methodology for these reductions is described in Watson et al. (2008) and summarised below.

The focus of the reductions to the full CRI v2 was on reducing the number of species and reactions representing anthropogenically emitted VOC, as on a global

Table 2.3: Summary of the CRI v2 and its five reduced variants. Data from Table 1 in Watson et al. (2008).

CRI version	v2	v2-R1	v2-R2	v2-R3	v2-R4	v2-R5
Primary VOCs	115	67	55	42	33	22
Species ^a	434(4361)	373(3466)	352(3099)	296(2649)	219(1983)	195(1244)
Reactions ^a	1183(12775)	1012(10150)	988(9099)	882(7833)	643(5884)	555(3670)

^a Data in brackets represents the number of species and reactions required to degrade the same VOCs in the MCM v3.1.

scale these VOC are less significant than biogenically emitted VOC. The primary VOC represented by the full CRI v2 were reduced into lumped species based upon two methods, first by re-distributing VOCs of minor importance into lumped mechanism species that represent the chemistry of separate functional classes (alkane, alkene, aromatic, alcohol/ether, aldehyde, ketone, ester/acid). POCPs of the primary VOC being lumped into mechanism species were used to determine the ozone production from the primary VOC and then select the appropriate mechanism species. This approach created three reduced variants (CRI v2-R1, CRI v2-R2 and CRI v2-R3), with progressively increased lumping of the primary VOC (Watson et al., 2008).

The second approach to reducing the CRI v2 chemistry involved stricter reductions by using definitions of individual VOC emissions from the Global Emissions Inventory Activity (GEIA). Again, POCP values of the individual VOC were used to assign the lumped mechanism species. This approach produced the two most reduced variants of the CRI v2—CRI v2-R4 and CRI v2-R5, where the latter is the most reduced form of the CRI v2 (Watson et al., 2008). A summary of the five reduced variants of the CRI v2 compared to the full CRI v2 is presented in Table 2.3.

2.2.3 Lumped Molecule Chemical Mechanisms

Lumped molecule chemical mechanisms reduce atmospheric chemistry by aggregating primary VOC into mechanism species; this is the most common technique used when developing a reduced chemical mechanism. Different chemical mechanisms use different approaches when creating these mechanism species that are used represent a multitude of primary VOC. Typically NMVOC, such as isoprene, ethane and ethene, that make up a large fraction of NMVOC emissions are represented by dedicated (explicit) species and mechanism species are used to represent specific groups of NMVOC. These lumped mechanism species typically represent NMVOC based on functional group or OH-reactivity. Table 2.2 lists the lumped-molecule chemical mechanisms used in this study and Table 2.4 provides further information about these chemical mechanisms.

Table 2.4: Explicitness of each of the lumped-molecule chemical mechanisms listed in Table 2.2

Chemical Mechanism	Number of Primary VOC	Number of Species	Number of Reactions
MOZART-4	20	85	157
RADM2	21	63	157
RACM	25	77	237
RACM2	40	120	363

MOZART

The Model for OZone and Related chemical Tracers (MOZART) chemical mechanism is an example of a lumped molecule chemical mechanism used in global and regional 3-D models. MOZART was developed for global chemical transport models and describes chemical processes within the boundary layer, free troposphere and stratosphere. MOZART-4 (Emmons et al., 2010) is the version used in this study and includes updates to the tropospheric chemistry from the previous MOZART-2 version (Horowitz et al., 2003); MOZART-3 (Kinnison et al., 2007) provided updated stratospheric chemistry.

MOZART-4 represents organic VOCs of methane, ethane, propane, ethene, propene, isoprene and formaldehyde by explicit species. Lumped mechanism species, BIGALK, BIGENE and TOLUENE, are used to represent alkanes and alkenes with four or more carbon atoms and all aromatic VOC (Emmons et al., 2010). Thus, the lumping species used by MOZART are based on the functionality of the VOC. There are no mechanism species representing emissions of esters, ethers or chlorinated NMVOC, when representing emissions of these less-reactive NMVOC are added to the BIGALK mechanism species as this has the slowest OH-reactivity.

MOZART-4 is also capable of representing aerosol chemistry and directly calculating both photolysis and dry deposition rates. For the purpose of this study, we were only interested in gas-phase chemical processes occurring with the boundary layer and so all processes relating to stratospheric, free troposphere and aerosol processes were not used. We also used the MCM approach to calculating photolysis and dry deposition rates.

RADM2

One of the older lumped molecule, but still widely used, chemical mechanisms is the second version of the Regional Acid Deposition Model (RADM2)

originally described in Stockwell et al. (1990). RADM2 is typically used in regional modelling studies and the chemical mechanism has been used extensively since its inception.

The organic VOC methane, ethane, ethene, isoprene and formaldehyde are represented explicitly in RAMD2. RADM2 uses lumped mechanism species to represent many VOC based upon the OH-reactivity and functional group of the VOC. In particular, there are three mechanism species (HC3, HC5, HC8) representing three types of hydrocarbons based on their OH-reactivity. These three species are then used to not only represent alkanes, but also many other species – such as alcohols, ethers, chlorinated VOC – based on their OH-reactivity.

All alkenes having more than two carbons are represented by either OLT or OLI depending on the position of the double bond (OLT: terminal alkenes and OLI: internal alkenes). The exception to this is isoprene, whose degradation is treated by an explicit species, due to the importance of isoprene chemistry as it is globally the VOC with the most emissions.

Aromatic VOC are represented by TOL, XYL or CSL depending on whether their OH-reactivity is slow, fast or they are hydroxy-substituted. Carbonyls (aldehydes and ketones) and organic acids are also represented by lumped mechanism species. Typically the NMVOC having the least number of carbons (e.g. formaldehyde and formic acid) is represented by an explicit species and then all other species from that functional group are represented by a lumped species.

The reaction rate coefficients of the lumped mechanism species were obtained by using a weighted mean of all the rate coefficients of the organic species aggregated into the model species, this was done to account for the difference in reactivities between the model and chemical species. The secondary degradation of the lumped species is described by chemistry that takes into account all the known VOC that are represented by the lumped species.

RADM2 reduces the number of peroxy radicals that need to be represented by using an operator species (XO2) that converts NO to NO₂ in an attempt to replicate the ozone produced by NMVOC when represented by the mechanism species. Thus, XO2 is one such mechanism species that appears in the secondary degradation of most of the lumped mechanism species. Another way of reducing the number of peroxy radicals is that only reactions of RO₂ with HO₂, CH₃O₂ and CH₃CO₃ are included as these are the most abundant RO₂.

RACM

Stockwell et al. (1997) describes the Regional Atmospheric Chemistry Mechanism (RACM) which is an updated to the RADM2 chemical mechanism. RACM includes lumped mechanism species not included in RADM2 such as API and LIM to represent cyclic terpenes with one double bond and all other cyclic terpenes.

Once again, the primary VOC are grouped into lumped mechanism species based upon functional group similarity and OH radical reactivity. The final mechanism species was determined by first grouping hundreds of anthropogenic VOCs into 32 emission categories and then finally aggregating into the final 16 lumped mechanism species.

The secondary chemistry of many of the lumped mechanism species included in both RADM2 and RACM was extensively updated which meant the inclusion of many new and additional mechanism species produced during the degradation of these lumped primary species. These product species are calculated as a weighted mean of the product yields of all the chemical species represented by the model species, where the individual yields are taken from literature.

The same approach to representing RO_2 - RO_2 reactions as used in RADM2 is used in RACM. Further details for calculating the reaction rate coefficients are described in Kirchner and Stockwell (1996).

RACM2

RACM was further extended and updated to RACM2, described in Goliff et al. (2013), once again the main updates included more lumped mechanism species to represent primary VOC emissions as well as updates to the secondary chemistry of lumped mechanism species. Alkane and alkene chemistry is largely unchanged from RACM except for some updates to reaction rate coefficients. Moreover, there were no major changes to the approach used when describing gas-phase chemistry from RADM2 or RACM.

Aromatic VOC and subsequent secondary chemistry was overhauled in RACM2 from RACM. RACM2 represents aromatic VOC by eight mechanism species instead of three species as in RACM, with explicit representation of benzene and each xylene isomer having its own mechanism species. The secondary chemistry of the aromatic VOC was updated to be similar to that of the MCM, with differences arising from the different treatments of gas-phase chemistry in the MCM and RACM2. The

Table 2.5: Carbon bonds and mechanism species represented in CBM-IV and CB05.

Mechanism Species	Carbon Bond
PAR	C–C
OLE	C=C
ALD2	C=O

main difference is the different treatment of $\text{RO}_2\text{-RO}_2$ reactions.

Acetone and methyl ethyl ketone (MEK) are now treated as separate species rather than being represent as a single mechanism species, KET, in RADM2 and RACM. Alcohols are now also represented in RACM2, whereas in the previous versions, alcohols were represented by HC3, HC5 or HC8.

2.2.4 Lumped Structure Chemical Mechanisms

The technique used by lumped-structure chemical mechanisms to reducing atmospheric chemistry is to express VOC emissions as permutations of building blocks that represent the structure of the emitted VOC. Thus, each lumped-structure chemical mechanism includes a number of these building blocks which are then emitted according to the initial VOC emissions being studied. The Carbon Bond mechanism is the most widely used lumped-structure chemical mechanism and in the first part of this thesis we have looked at the fourth version (CBM-IV, (Gery et al., 1989)) and the fifth version (CB05, (Yarwood et al., 2005)). Both Carbon Bond versions include mechanism species representing the different carbon bonds present in typically emitted VOC, the representation of the carbon bonds included in CBM-IV and CB05 are outlined in Table 2.5.

CBM-IV

The fourth version of the Carbon Bond mechanism was developed to represent the chemistry producing ozone in polluted urban conditions and is described in Gery et al. (1989). CBM-IV represents 20 organic species and requires 46 reactions to fully represent the secondary chemistry. Explicitly represented emitted NMVOC are those with the most significant emissions: isoprene, ethene and formaldehyde. In addition to the mechanism species listed in Table 2.5, there are mechanism species representing both slower and faster reacting aromatic VOC (TOL and XYL). Acetaldehyde (ALD2) is also represented as it is an important degradation product of the secondary chemistry from a number of VOC. CBM-IV uses an operator species

(XO2) to represent NO to NO₂ conversion by organic peroxy radical, similar to many lumped-molecule chemical mechanisms.

NMVOC emissions emitted by the mechanism species are described in Hogo and Gery (1989). For example, if heptane, having seven carbons each with a single bond, has emissions of 1×10^9 molecules cm⁻³ s⁻¹ then using the CBM-IV, these emissions would be represented by 7 PAR and thus PAR emissions would be 7×10^9 molecules cm⁻³ s⁻¹. Also, propene is represented as 1 OLE and 1 PAR and so emissions of 1×10^9 molecules cm⁻³ s⁻¹ would be emitted as 1×10^9 molecules cm⁻³ s⁻¹ of OLE and 1×10^9 molecules cm⁻³ s⁻¹ of PAR.

CB05

CBM-IV was updated to CB05, described in Yarwood et al. (2005), to include more species representing emitted VOC. CB05 now includes 99 organic reactions to represent the degradation of 37 organic species. Mechanism species for terpenes (TERP), ethane (ETHA), aldehydes with more than three carbons (ALDX), methanol (MEOH), ethanol (ETOH) and alkenes with both internal (IOLE) and external (OLE) double bonds were included.

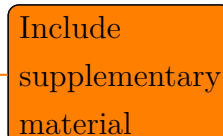
In addition to updating reaction rate constants and including more mechanism species to represent atmospheric chemistry more explicitly, the CB05 was also updated to include chemistry reflecting low-NO_x conditions. Thus reactions involving peroxide formation, a characteristic of low-NO_x conditions, were included in CB05.

2.3 Using the Chemical Mechanisms in MECCA

As outlined in Sect. 2.1.1, the MECCA boxmodel is based upon the KPP pre-processor and so required that all chemical mechanisms listed in Table 2.2 be written in the KPP format. The KPP format of each chemical mechanism was either obtained from the WRF/Chem (Grell et al., 2005) model, which includes KPP files of RADM2, RACM and CBM-IV for use within the model. For all the other chemical mechanisms, the chemistry published in the original reference were adapted to the KPP format.

Some changes were made to the original chemistry specified by each chemical mechanism. Firstly, the inorganic chemistry of the MCM v3.2 was used in each

chemical mechanism in order to focus on differences between chemical mechanisms of their representation of the secondary degradation chemistry of emitted NMVOC. Other changes included adopting the MCM v3.2 approaches to photolysis and peroxy-peroxy reactions, a more detailed description of these changes are found in the supplementary material of the first paper of this thesis (Chap. 6).



Include
supplementary
material

Chapter 3

Presentation of Papers

This chapter will outline the main findings in each of the scientific papers that were published as part of the PhD.

3.1 Paper 1: A comparison of chemical mechanisms using tagged ozone production potential (TOPP) analysis

Published: J. Coates and T. M. Butler. A comparison of chemical mechanisms using tagged ozone production potential (TOPP) analysis. *Atmospheric Chemistry and Physics*, 15(15):8795–8808, 2015. doi:10.5194/acp-15-8795-2015. URL <http://www.atmos-chem-phys.net/15/8795/2015/>.

The first paper described a box modelling study in which the secondary chemistry represented in many reduced chemical mechanisms (Table) for VOC

 typical of urban environments (Table 2 of the article) were compared to the detailed MCM chemical mechanisms. The research question addressed in this paper was to verify whether these different representations of this secondary chemistry influence ozone production.

The degradation of each VOC prescribed in each chemical mechanism was “tagged” so that the O_x production, a proxy for O_3 production, could be attributed to the individual VOC sources. Tagging the chemical mechanisms involved labelling every organic degradation product from a VOC with the name of the emitted VOC,

thus each VOC has a separate set of reactions fully describing its degradation until the final products, CO_2 and H_2O , are produced.

The ozone mixing ratios from reduced chemical mechanisms were generally lower than the mixing ratios from the reference MCM chemical mechanisms on the first two days of the simulations. The VOC degradation prescribed in CRI v2, a lumped-intermediate mechanism, produced the most similar amounts of O_x to the MCM v3.2 for each VOC. Thus, the approach of using lumped-intermediate species whose degradation are based upon more detailed chemical mechanisms is preferable when developing future chemical mechanisms.

Many VOC are broken down into smaller-sized degradation products faster on the first day in reduced chemical mechanisms than the MCM v3.2 leading to lower amounts of larger-sized degradation products that can further degrade and produce O_x . Thus, many VOC in reduced chemical mechanisms produce a lower maximum of O_x than the MCM v3.2 ultimately leading to lower O_3 mixing ratios from the reduced chemical mechanisms compared to the MCM v3.2.

Reactive VOC, such as unsaturated aliphatic and aromatic VOC, produce maximum O_x on the first day of the simulations. Unsaturated aliphatic VOC produce similar amounts of O_x on the first day between mechanisms; differences in O_x production arise when mechanism species are used to represent individual VOC. Large inter-mechanism differences in O_x production result from the degradation of aromatic VOC on the first day due to the faster break down of the mechanism species representing aromatic VOC in reduced chemical mechanisms.

The less-reactive alkanes produce maximum O_x on the second day of simulations and this maximum is lower in each reduced chemical mechanism than the MCM v3.2 due to the faster break down of alkanes into smaller sized degradation products on the first day. The lower maximum in O_x production during alkane degradation in reduced mechanisms would lead to an underestimation of the O_3 levels downwind of VOC emissions, and an underestimation of the VOC contribution to tropospheric background O_3 when using reduced mechanisms in regional or global modelling studies.

3.2 Paper 2:

3.3 Paper 3:

Chapter 4

Overall Discussion and Conclusions

Chapter 5

Summary and Zusammenfassung

References

J. Abbatt, C. George, M. Melamed, P. Monks, S. Pandis, and Y. Rudich. New directions: Fundamentals of atmospheric chemistry: Keeping a three-legged stool balanced. *Atmospheric Environment*, 48:390 – 391, 2014. ISSN 1352-2310. doi:<http://dx.doi.org/10.1016/j.atmosenv.2013.10.025>. URL <http://www.sciencedirect.com/science/article/pii/S1352231013007784>.

S. Archer-Nicholls, D. Lowe, S. Utembe, J. Allan, R. A. Zaveri, J. D. Fast, Ø. Hodnebrog, H. Denier van der Gon, and G. McFiggans. Gaseous chemistry and aerosol mechanism developments for version 3.5.1 of the online regional model, WRF-Chem. *Geoscientific Model Development*, 7(6):2557–2579, 2014. doi:10.5194/gmd-7-2557-2014. URL <http://www.geosci-model-dev.net/7/2557/2014/>.

R. Atkinson. Atmospheric chemistry of VOCs and NO_x. *Atmospheric Environment*, 34(12-14):2063–2101, 2000.

B. Aumont, S. Szopa, and S. Madronich. Modelling the evolution of organic carbon during its gas-phase tropospheric oxidation: development of an explicit model based on a self generating approach. *Atmospheric Chemistry and Physics*, 5(9):2497–2517, 2005. doi:10.5194/acp-5-2497-2005. URL <http://www.atmos-chem-phys.net/5/2497/2005/>.

C. Bloss, V. Wagner, M. E. Jenkin, R. Vollamer, W. J. Bloss, J. D. Lee, D. E. Heard, K. Wirtz, M. Martin-Reviejo, G. Rea, J. C. Wenger, and M. J. Pilling. Development of a detailed chemical mechanism (MCMv3.1) for the atmospheric oxidation of aromatic hydrocarbons. *Atmospheric Chemistry and Physics*, 5:641–664, 2005.

T. Butler, M. Lawrence, D. Taraborrelli, and J. Lelieveld. Multi-day ozone production potential of volatile organic compounds calculated with a tagging approach. *Atmospheric Environment*, 45(24):4082 – 4090, 2011. ISSN 1352-2310. doi:<http://dx.doi.org/10.1016/j.atmosenv.2011.03.040>. URL <http://www.sciencedirect.com/science/article/pii/S1352231011003001>.

L. Camalier, W. Cox, and P. Dolwick. The effects of meteorology on ozone in urban areas and their use in assessing ozone trends. *Atmospheric Environment*, 41(33):7127 – 7137, 2007. ISSN 1352-2310. doi:<http://dx.doi.org/10.1016/j.atmosenv.2007.04.061>. URL <http://www.sciencedirect.com/science/article/pii/S1352231007004165>.

W. P. L. Carter. Development of a Database for Chemical Mechanism Assignments for Volatile Organic Emissions. *Journal of the Air & Waste Management Association*, 0, 2015. doi:10.1080/10962247.2015.1013646. URL <http://dx.doi.org/10.1080/10962247.2015.1013646>.

J. Coates and T. M. Butler. A comparison of chemical mechanisms using tagged ozone production potential (TOPP) analysis. *Atmospheric Chemistry and Physics*, 15(15):8795–8808, 2015. doi:10.5194/acp-15-8795-2015. URL <http://www.atmos-chem-phys.net/15/8795/2015/>.

V. Damian, A. Sandu, M. Damian, F. Potra, and G. R. Carmichael. The kinetic preprocessor KPP-a software environment for solving chemical kinetics. *Computers & Chemical Engineering*, 26(11):1567 – 1579, 2002. ISSN 0098-1354. doi:[http://dx.doi.org/10.1016/S0098-1354\(02\)00128-X](http://dx.doi.org/10.1016/S0098-1354(02)00128-X). URL <http://www.sciencedirect.com/science/article/pii/S009813540200128X>.

J. P. Dawson, P. J. Adams, and S. N. Pandis. Sensitivity of ozone to summertime climate in the eastern USA: A modeling case study . *Atmospheric Environment*, 41(7):1494 – 1511, 2007. ISSN 1352-2310. doi:<http://dx.doi.org/10.1016/j.atmosenv.2006.10.033>. URL <http://www.sciencedirect.com/science/article/pii/S1352231006010223>.

J. P. Dawson, P. N. Racherla, B. H. Lynn, P. J. Adams, and S. N. Pandis. Impacts of climate change on regional and urban air quality in the eastern united states: Role of meteorology. *Journal of Geophysical Research: Atmospheres*, 114(D5), 2009. ISSN 2156-2202. doi:10.1029/2008JD009849. URL <http://dx.doi.org/10.1029/2008JD009849>. D05308.

H. Denier van der Gon, C. Hendriks, J. Kuenen, A. Segers, and A. Visschedijk. Description of current temporal emission patterns and sensitivity of predicted AQ for temporal emission patterns. Technical Report EU FP7 MACC report: D_D-EMIS_1.3, TNO, 2011.

R. M. Doherty, O. Wild, D. T. Shindell, G. Zeng, I. A. MacKenzie, W. J. Collins, A. M. Fiore, D. S. Stevenson, F. J. Dentener, M. G. Schultz, P. Hess, R. G. Derwent, and T. J. Keating. Impacts of climate change on surface ozone and intercontinental ozone

pollution: A multi-model study. *Journal of Geophysical Research: Atmospheres*, 118(9):3744–3763, 2013. ISSN 2169-8996. doi:10.1002/jgrd.50266. URL <http://dx.doi.org/10.1002/jgrd.50266>.

EEA. Air quality in Europe - 2013 report. Technical Report 9/2013, European Environmental Agency, 2013.

EEA. Air quality in Europe - 2015 report. Technical Report 5/2015, European Environmental Agency, 2015.

L. K. Emmons, S. Walters, P. G. Hess, J.-F. Lamarque, G. G. Pfister, D. Fillmore, C. Granier, A. Guenther, D. Kinnison, T. Laepple, J. Orlando, X. Tie, G. Tyndall, C. Wiedinmyer, S. L. Baughcum, and S. Kloster. Description and evaluation of the Model for Ozone and Related chemical Tracers, version 4 (MOZART-4). *Geoscientific Model Development*, 3(1):43–67, 2010. doi:10.5194/gmd-3-43-2010. URL <http://www.geosci-model-dev.net/3/43/2010/>.

V. Eyring, J.-F. Lamarque, P. Hess, F. Arfeuille, K. Bowman, M. P. Chipperfield, B. Duncan, A. Fiore, A. Gettelman, M. A. Giorgetta, C. Granier, M. Hegglin, D. Kinnison, M. Kunze, U. Langematz, B. Luo, R. Martin, K. Matthes, P. A. Newman, T. Peter, A. Robock, T. Ryerson, A. Saiz-Lopez, R. Salawitch, M. Schultz, T. G. Shepherd, D. Shindell, J. Staehelin, S. Tegtmeier, L. Thomason, S. Tilmes, J.-P. Vernier, D. W. Waugh, , and P. J. Young. Overview of IGAC/SPARC Chemistry-Climate Model Initiative (CCMI) Community Simulations in Support of Upcoming Ozone and Climate Assessments. *SPARC Newsletter*, 40:48–66, 2013. ISSN 1245-4680. URL <http://www.met.reading.ac.uk/ccmi/>.

M. W. Gery, G. Z. Whitten, J. P. Killus, and M. C. Dodge. A photochemical kinetics mechanism for urban and regional scale computer modeling. *Journal of Geophysical Research*, 94(D10):12,925–12,956, 1989.

W. S. Goliff, W. R. Stockwell, and C. V. Lawson. The regional atmospheric chemistry mechanism, version 2. *Atmospheric Environment*, 68:174 – 185, 2013. ISSN 1352-2310. doi:<http://dx.doi.org/10.1016/j.atmosenv.2012.11.038>. URL <http://www.sciencedirect.com/science/article/pii/S1352231012011065>.

G. Grell, S. Peckham, R. Schmitz, S. McKeen, G. Frost, W. Skamarock, and B. Eder. Fully coupled "online" chemistry within the WRF model. *Atmospheric Environment*, 39(37):6957–6975, 2005.

S. Grice, J. Stedman, A. Kent, M. Hobson, J. Norris, J. Abbott, and S. Cooke. Recent trends and projections of primary no₂ emissions in europe. *Atmospheric Environment*, 43(13):2154 – 2167, 2009. ISSN

1352-2310. doi:<http://dx.doi.org/10.1016/j.atmosenv.2009.01.019>. URL <http://www.sciencedirect.com/science/article/pii/S1352231009000508>.

A. B. Guenther, X. Jiang, C. L. Heald, T. Sakulyanontvittaya, T. Duhl, L. K. Emmons, and X. Wang. The Model of Emissions of Gases and Aerosols from Nature version 2.1 (MEGAN2.1): an extended and updated framework for modeling biogenic emissions. *Geoscientific Model Development*, 5(6):1471–1492, 2012. doi:10.5194/gmd-5-1471-2012. URL <http://www.geosci-model-dev.net/5/1471/2012/>.

D. W. Gunz and M. R. Hoffmann. Atmospheric chemistry of peroxides: a review. *Atmospheric Environment. Part A. General Topics*, 24(7):1601 – 1633, 1990. ISSN 0960-1686. doi:[http://dx.doi.org/10.1016/0960-1686\(90\)90496-A](http://dx.doi.org/10.1016/0960-1686(90)90496-A). URL <http://www.sciencedirect.com/science/article/pii/096016869090496A>.

D. A. Hauglustaine, G. P. Brasseur, S. Walters, P. J. Rasch, J.-F. Müller, L. K. Emmons, and M. A. Carroll. MOZART, a global chemical transport model for ozone and related chemical tracers 2. Model results and evaluation. *Journal of Geophysical Research*, 103(D21):28,291–28,335, 1998.

H. Hogo and M. Gery. USER'S GUIDE FOR EXECUTING OZIPM-4 (OZONE ISOPLETH PLOTTING WITH OPTIONAL MECHANISMS, VERSION 4) WITH CBM-IV (CARBON-BOND MECHANISMS-IV) OR OPTIONAL MECHANISMS. VOLUME 1. DESCRIPTION OF THE OZONE ISOPLETH PLOTTING PACKAGE. VERSION 4. Technical report, U.S. Environmental Protection Agency, 1989.

C. D. Holmes, M. J. Prather, O. A. Søvde, and G. Myhre. Future methane, hydroxyl, and their uncertainties: key climate and emission parameters for future predictions. *Atmospheric Chemistry and Physics*, 13(1):285–302, 2013. doi:10.5194/acp-13-285-2013. URL <http://www.atmos-chem-phys.net/13/285/2013/>.

L. W. Horowitz, S. Walters, D. L. Mauzerall, L. K. Emmons, P. J. Rasch, C. Granier, X. Tie, J.-F. Lamarque, M. G. Schultz, G. S. Tyndall, J. J. Orlando, and G. P. Brasseur. A global simulation of tropospheric ozone and related tracers: Description and evaluation of MOZART, version 2. *Journal of Geophysical Research: Atmospheres*, 108(D24), 2003. ISSN 2156-2202. doi:10.1029/2002JD002853. URL <http://dx.doi.org/10.1029/2002JD002853>. 4784.

IARC. Outdoor air pollution a leading environmental cause of cancer deaths. https://www.iarc.fr/en/media-centre/iarcnews/pdf/pr221_E.pdf, 2013. [Online; accessed 31-December-2015].

D. J. Jacob and D. A. Winner. Effect of climate change on air quality. *Atmospheric Environment*, 43(1):51 – 63, 2009. ISSN 1352-2310. doi:<http://dx.doi.org/10.1016/j.atmosenv.2008.09.051>. URL <http://www.sciencedirect.com/science/article/pii/S1352231008008571>.

Atmospheric Environment - Fifty Years of Endeavour.

M. Jenkin, L. Watson, S. Utembe, and D. Shallcross. A Common Representative Intermediates (CRI) mechanism for VOC degradation. Part 1: Gas phase mechanism development. *Atmospheric Environment*, 42(31):7185 – 7195, 2008. ISSN 1352-2310. doi:<http://dx.doi.org/10.1016/j.atmosenv.2008.07.028>. URL <http://www.sciencedirect.com/science/article/pii/S1352231008006742>.

M. E. Jenkin and K. C. Clemitshaw. Ozone and other secondary photochemical pollutants: Chemical processes governing their formation in the planetary boundary layer. *Atmospheric Environment*, 34(16):2499–2527, 2000.

M. E. Jenkin, S. M. Saunders, and M. J. Pilling. The tropospheric degradation of volatile organic compounds: a protocol for mechanism development. *Atmospheric Environment*, 31(1):81 – 104, 1997. ISSN 1352-2310. doi:[http://dx.doi.org/10.1016/S1352-2310\(96\)00105-7](http://dx.doi.org/10.1016/S1352-2310(96)00105-7). URL <http://www.sciencedirect.com/science/article/pii/S1352231096001057>.

M. E. Jenkin, S. M. Saunders, V. Wagner, and M. J. Pilling. Protocol for the development of the Master Chemical Mechanism, MCM v3 (Part B): tropospheric degradation of aromatic volatile organic compounds. *Atmospheric Chemistry and Physics*, 3(1):181–193, 2003. doi:10.5194/acp-3-181-2003. URL <http://www.atmos-chem-phys.net/3/181/2003/>.

D. E. Kinnison, G. P. Brasseur, S. Walters, R. R. Garcia, D. R. Marsh, F. Sassi, V. L. Harvey, C. E. Randall, L. Emmons, J. F. Lamarque, P. Hess, J. J. Orlando, X. X. Tie, W. Randel, L. L. Pan, A. Gettelman, C. Granier, T. Diehl, U. Niemeier, and A. J. Simmons. Sensitivity of chemical tracers to meteorological parameters in the MOZART-3 chemical transport model. *Journal of Geophysical Research: Atmospheres*, 112(D20), 2007. ISSN 2156-2202. doi:10.1029/2006JD007879. URL <http://dx.doi.org/10.1029/2006JD007879>. D20302.

F. Kirchner and W. R. Stockwell. Effect of peroxy radical reactions on the predicted concentrations of ozone, nitrogenous compounds, and radicals. *Journal of Geophysical Research: Atmospheres*, 101(D15):21007–21022, 1996. ISSN 2156-2202. doi:10.1029/96JD01519. URL <http://dx.doi.org/10.1029/96JD01519>.

S. Kirschke, P. Bousquet, P. Ciais, M. Saunois, J. G. Canadell, E. J. Dlugokencky, P. Bergamaschi, D. Bergmann, D. R. Blake, L. Bruhwiler, P. Cameron-Smith,

S. Castaldi, F. Chevallier, L. Feng, A. Fraser, M. Heimann, E. L. Hodson, S. Houweling, B. Josse, P. J. Fraser, P. B. Krummel, J.-F. Lamarque, R. L. Langenfelds, C. Le Quere, V. Naik, S. O'Doherty, P. I. Palmer, I. Pison, D. Plummer, B. Poulter, R. G. Prinn, M. Rigby, B. Ringeval, M. Santini, M. Schmidt, D. T. Shindell, I. J. Simpson, R. Spahni, L. P. Steele, S. A. Strode, K. Sudo, S. Szopa, G. R. van der Werf, A. Voulgarakis, M. van Weele, R. F. Weiss, J. E. Williams, and G. Zeng. Three decades of global methane sources and sinks. *Nature Geoscience*, 6(10):813–823, 2013. doi:10.1038/ngeo1955. URL <http://dx.doi.org/10.1038/ngeo1955>.

L. I. Kleinman. Seasonal Dependence of Boundary Layer Peroxide Concentration: The Low and High NO_x Regimes. *Journal of Geophysical Research*, 96(D11):20,721–20,733, 1991.

L. I. Kleinman. Low and high NO_x tropospheric photochemistry. *Journal of Geophysical Research*, 99(D8):16,831–16,838, 1994.

D. Kubistin, H. Harder, M. Martinez, M. Rudolf, R. Sander, H. Bozem, G. Eerdekens, H. Fischer, C. Gurk, T. Klüpfel, R. Königstedt, U. Parchatka, C. L. Schiller, A. Stickler, D. Taraborrelli, J. Williams, and J. Lelieveld. Hydroxyl radicals in the tropical troposphere over the Suriname rainforest: comparison of measurements with the box model MECCA. *Atmospheric Chemistry and Physics*, 10(19):9705–9728, 2010. doi:10.5194/acp-10-9705-2010. URL <http://www.atmos-chem-phys.net/10/9705/2010/>.

J. J. P. Kuenen, A. J. H. Visschedijk, M. Jozwicka, and H. A. C. Denier van der Gon. TNO-MACC_II emission inventory; a multi-year (2003–2009) consistent high-resolution european emission inventory for air quality modelling. *Atmospheric Chemistry and Physics*, 14(20):10963–10976, 2014. doi:10.5194/acp-14-10963-2014. URL <http://www.atmos-chem-phys.net/14/10963/2014/>.

J.-F. Lamarque, T. C. Bond, V. Eyring, C. Granier, A. Heil, Z. Klimont, D. Lee, C. Liousse, A. Mieville, B. Owen, M. G. Schultz, D. Shindell, S. J. Smith, E. Stehfest, J. Van Aardenne, O. R. Cooper, M. Kainuma, N. Mahowald, J. R. McConnell, V. Naik, K. Riahi, and D. P. van Vuuren. Historical (1850–2000) gridded anthropogenic and biomass burning emissions of reactive gases and aerosols: methodology and application. *Atmospheric Chemistry and Physics*, 10(15):7017–7039, 2010. doi:10.5194/acp-10-7017-2010. URL <http://www.atmos-chem-phys.net/10/7017/2010/>.

A. Laurent and M. Z. Hauschild. Impacts of NMVOC emissions on human health in European countries for 2000–2010: Use of sector-specific substance profiles. *Atmospheric Environment*, 85(0):247–255, 2014. ISSN

1352-2310. doi:10.1016/j.atmosenv.2013.11.060. URL <http://www.sciencedirect.com/science/article/pii/S1352231013009102>.

J. Lelieveld and F. J. Dentener. What controls tropospheric ozone? *Journal of Geophysical Research: Atmospheres*, 105(D3):3531–3551, 2000. ISSN 2156-2202. doi:10.1029/1999JD901011. URL <http://dx.doi.org/10.1029/1999JD901011>.

X. Li, F. Rohrer, T. Brauers, A. Hofzumahaus, K. Lu, M. Shao, Y. H. Zhang, and A. Wahner. Modeling of HCHO and CHOCHO at a semi-rural site in southern China during the PRIDE-PRD2006 campaign. *Atmospheric Chemistry and Physics*, 14(22):12291–12305, 2014. doi:10.5194/acp-14-12291-2014. URL <http://www.atmos-chem-phys.net/14/12291/2014/>.

A. S. M. Lourens, T. M. Butler, J. P. Beukes, P. G. van Zyl, G. D. Fourie, and M. G. Lawrence. Investigating atmospheric photochemistry in the Johannesburg-Pretoria megacity using a box model. *South African Journal of Science*, 112(1/2), 2016. URL <http://dx.doi.org/10.17159/sajs.2016/2015-0169>.

P. S. Monks. A review of the observations and origins of the spring ozone maximum. *Atmospheric Environment*, 34(21):3545 – 3561, 2000. ISSN 1352-2310. doi:[http://dx.doi.org/10.1016/S1352-2310\(00\)00129-1](http://dx.doi.org/10.1016/S1352-2310(00)00129-1). URL <http://www.sciencedirect.com/science/article/pii/S1352231000001291>.

P. S. Monks. Gas-phase radical chemistry in the troposphere. *Chem. Soc. Rev.*, 34:376–395, 2005. doi:10.1039/B307982C. URL <http://dx.doi.org/10.1039/B307982C>.

A. Nölscher, T. Butler, J. Auld, P. Veres, A. Muñoz, D. Taraborrelli, L. Vereecken, J. Lelieveld, and J. Williams. Using total OH reactivity to assess isoprene photooxidation via measurement and model. *Atmospheric Environment*, 89(0): 453–463, 2014. ISSN 1352-2310. doi:10.1016/j.atmosenv.2014.02.024. URL <http://www.sciencedirect.com/science/article/pii/S1352231014001204>.

N. Otero, J. Sillmann, J. L. Schnell, H. W. Rust, and T. Butler. Synoptic and meteorological drivers of extreme ozone concentrations over europe. *Environmental Research Letters*, 11(2):024005, 2016. URL <http://stacks.iop.org/1748-9326/11/i=2/a=024005>.

S. A. Penkett and K. A. Brice. The spring maximum of photo-oxidants in the Northern Hemisphere troposphere. *Nature*, 319:655–657, 1986.

S. E. Pusede, D. R. Gentner, P. J. Wooldridge, E. C. Browne, A. W. Rollins, K.-E. Min, A. R. Russell, J. Thomas, L. Zhang, W. H. Brune, S. B. Henry, J. P.

DiGangi, F. N. Keutsch, S. A. Harrold, J. A. Thornton, M. R. Beaver, J. M. St. Clair, P. O. Wennberg, J. Sanders, X. Ren, T. C. VandenBoer, M. Z. Markovic, A. Guha, R. Weber, A. H. Goldstein, and R. C. Cohen. On the temperature dependence of organic reactivity, nitrogen oxides, ozone production, and the impact of emission controls in San Joaquin Valley, California. *Atmospheric Chemistry and Physics*, 14(7):3373–3395, 2014. doi:10.5194/acp-14-3373-2014. URL <http://www.atmos-chem-phys.net/14/3373/2014/>.

S. E. Pusede, A. L. Steiner, and R. C. Cohen. Temperature and Recent Trends in the Chemistry of Continental Surface Ozone. *Chemical Reviews*, 115(10):3898–3918, 2015. doi:10.1021/cr5006815. URL <http://dx.doi.org/10.1021/cr5006815>.

B. Qi, Y. Kanaya, A. Takami, S. Hatakeyama, S. Kato, Y. Sadanaga, H. Tanimoto, and Y. Kajii. Diurnal peroxy radical chemistry at a remote coastal site over the sea of Japan. *Journal of Geophysical Research: Atmospheres*, 112(D17), 2007. ISSN 2156-2202. doi:10.1029/2006JD008236. URL <http://dx.doi.org/10.1029/2006JD008236>. D17306.

A. Rickard, J. Young, M. J. Pilling, M. E. Jenkin, S. Pascoe, and S. M. Saunders. The Master Chemical Mechanism Version MCM v3.2. <http://mcm.leeds.ac.uk/MCMv3.2/>, 2015. [Online; accessed 25-March-2015].

A. Russell and R. Dennis. NARSTO critical review of photochemical models and modeling. *Atmospheric Environment*, 34(12–14):2283 – 2324, 2000. ISSN 1352-2310. doi:[http://dx.doi.org/10.1016/S1352-2310\(99\)00468-9](http://dx.doi.org/10.1016/S1352-2310(99)00468-9). URL <http://www.sciencedirect.com/science/article/pii/S1352231099004689>.

R. Sander, A. Kerkweg, P. Jöckel, and J. Lelieveld. Technical note: The new comprehensive atmospheric chemistry module mecca. *Atmospheric Chemistry and Physics*, 5(2):445–450, 2005. doi:10.5194/acp-5-445-2005. URL <http://www.atmos-chem-phys.net/5/445/2005/>.

A. Sandu, J. Verwer, J. Blom, E. Spee, G. Carmichael, and F. Potra. Benchmarking stiff ode solvers for atmospheric chemistry problems II: Rosenbrock solvers. *Atmospheric Environment*, 31(20):3459 – 3472, 1997a. ISSN 1352-2310. doi:[http://dx.doi.org/10.1016/S1352-2310\(97\)83212-8](http://dx.doi.org/10.1016/S1352-2310(97)83212-8). URL <http://www.sciencedirect.com/science/article/pii/S1352231097832128>.

A. Sandu, J. Verwer, M. V. Loon, G. Carmichael, F. Potra, D. Dabdub, and J. Seinfeld. Benchmarking stiff ode solvers for atmospheric chemistry problems-I. implicit vs explicit . *Atmospheric Environment*, 31(19):3151 – 3166, 1997b. ISSN 1352-2310. doi:[http://dx.doi.org/10.1016/S1352-2310\(97\)00059-9](http://dx.doi.org/10.1016/S1352-2310(97)00059-9). URL <http://www.sciencedirect.com/science/article/pii/S1352231097000599>.

S. M. Saunders, M. E. Jenkin, R. G. Derwent, and M. J. Pilling. Protocol for the development of the Master Chemical Mechanism, MCM v3 (Part A): tropospheric degradation of non-aromatic volatile organic compounds. *Atmospheric Chemistry and Physics*, 3(1):161–180, 2003. doi:10.5194/acp-3-161-2003. URL <http://www.atmos-chem-phys.net/3/161/2003/>.

J. H. Seinfeld and S. N. Pandis. *Atmospheric Chemistry and Physics: From Air Pollution to Climate Change*. John Wiley & Sons Inc, New York, second edition, 2006. ISBN 978-0-471-72018-8.

S. Sillman and P. J. Samson. Impact of temperature on oxidant photochemistry in urban, polluted rural and remote environments. *Journal of Geophysical Research: Atmospheres*, 100(D6):11497–11508, 1995. ISSN 2156-2202. doi:10.1029/94JD02146. URL <http://dx.doi.org/10.1029/94JD02146>.

W. R. Stockwell, P. Middleton, J. S. Chang, and X. Tang. The second generation regional acid deposition model chemical mechanism for regional air quality modeling. *Journal of Geophysical Research: Atmospheres*, 95(D10):16343–16367, 1990. ISSN 2156-2202. doi:10.1029/JD095iD10p16343. URL <http://dx.doi.org/10.1029/JD095iD10p16343>.

W. R. Stockwell, F. Kirchner, M. Kuhn, and S. Seefeld. A new mechanism for regional atmospheric chemistry modeling. *Journal of Geophysical Research: Atmospheres*, 102(D22):25847–25879, 1997. ISSN 2156-2202. doi:10.1029/97JD00849. URL <http://dx.doi.org/10.1029/97JD00849>.

E. von Schneidmesser, P. S. Monks, V. Gros, J. Gauduin, and O. Sanchez. How important is biogenic isoprene in an urban environment? a study in london and paris. *Geophysical Research Letters*, 38(19), 2011. ISSN 1944-8007. doi:10.1029/2011GL048647. URL <http://dx.doi.org/10.1029/2011GL048647>. L19804.

E. von Schneidmesser, P. S. Monks, J. D. Allan, L. Bruhwiler, P. Forster, D. Fowler, A. Lauer, W. T. Morgan, P. Paasonen, M. Righi, K. Sindelarova, and M. A. Sutton. Chemistry and the Linkages between Air Quality and Climate Change. *Chemical Reviews*, 2015. doi:10.1021/acs.chemrev.5b00089. URL <http://dx.doi.org/10.1021/acs.chemrev.5b00089>. PMID: 25926133.

L. Watson, D. Shallcross, S. Utembe, and M. Jenkin. A Common Representative Intermediates (CRI) mechanism for VOC degradation. Part 2: Gas phase mechanism reduction. *Atmospheric Environment*, 42(31):7196 – 7204, 2008. ISSN 1352-2310. doi:http://dx.doi.org/10.1016/j.atmosenv.2008.07.034. URL <http://www.sciencedirect.com/science/article/pii/S1352231008006845>.

World Meteorological Organisation. Scientific Assessment of Ozone Depletion: 2010. Technical Report 516 pp., World Meteorological Organisation, Geneva, Switzerland, March 2011.

Z.-Q. Xie, R. Sander, U. Pöschl, and F. Slemr. Simulation of atmospheric mercury depletion events (AMDEs) during polar springtime using the MECCA box model. *Atmospheric Chemistry and Physics*, 8(23):7165–7180, 2008. doi:10.5194/acp-8-7165-2008. URL <http://www.atmos-chem-phys.net/8/7165/2008/>.

G. Yarwood, S. Rao, M. Yocke, and G. Z. Whitten. Updates to the Carbon Bond Chemical Mechanism: CB05. Technical report, U. S Environmental Protection Agency, 2005.

P. J. Young, A. T. Archibald, K. W. Bowman, J.-F. Lamarque, V. Naik, D. S. Stevenson, S. Tilmes, A. Voulgarakis, O. Wild, D. Bergmann, P. Cameron-Smith, I. Cionni, W. J. Collins, S. B. Dalsøren, R. M. Doherty, V. Eyring, G. Faluvegi, L. W. Horowitz, B. Josse, Y. H. Lee, I. A. MacKenzie, T. Nagashima, D. A. Plummer, M. Righi, S. T. Rumbold, R. B. Skeie, D. T. Shindell, S. A. Strode, K. Sudo, S. Szopa, and G. Zeng. Pre-industrial to end 21st century projections of tropospheric ozone from the atmospheric chemistry and climate model intercomparison project (accmip). *Atmospheric Chemistry and Physics*, 13(4):2063–2090, 2013. doi:10.5194/acp-13-2063-2013. URL <http://www.atmos-chem-phys.net/13/2063/2013/>.

Chapter 6

Paper 1: A comparison of
chemical mechanisms using tagged
ozone production potential
(TOPP) analysis



A comparison of chemical mechanisms using tagged ozone production potential (TOPP) analysis

J. Coates and T. M. Butler

Institute for Advanced Sustainability Studies, Potsdam, Germany

Correspondence to: J. Coates (jane.coates@iass-potsdam.de)

Received: 10 April 2015 – Published in Atmos. Chem. Phys. Discuss.: 29 April 2015

Revised: 23 July 2015 – Accepted: 24 July 2015 – Published: 10 August 2015

Abstract. Ground-level ozone is a secondary pollutant produced photochemically from reactions of NO_x with peroxy radicals produced during volatile organic compound (VOC) degradation. Chemical transport models use simplified representations of this complex gas-phase chemistry to predict O_3 levels and inform emission control strategies. Accurate representation of O_3 production chemistry is vital for effective prediction. In this study, VOC degradation chemistry in simplified mechanisms is compared to that in the near-explicit Master Chemical Mechanism (MCM) using a box model and by “tagging” all organic degradation products over multi-day runs, thus calculating the tagged ozone production potential (TOPP) for a selection of VOCs representative of urban air masses. Simplified mechanisms that aggregate VOC degradation products instead of aggregating emitted VOCs produce comparable amounts of O_3 from VOC degradation to the MCM. First-day TOPP values are similar across mechanisms for most VOCs, with larger discrepancies arising over the course of the model run. Aromatic and unsaturated aliphatic VOCs have the largest inter-mechanism differences on the first day, while alkanes show largest differences on the second day. Simplified mechanisms break VOCs down into smaller-sized degradation products on the first day faster than the MCM, impacting the total amount of O_3 produced on subsequent days due to secondary chemistry.

gen oxides ($\text{NO}_x = \text{NO} + \text{NO}_2$) in the presence of sunlight (Atkinson, 2000).

Background O_3 concentrations have increased during the last several decades due to the increase of overall global anthropogenic emissions of O_3 precursors (HTAP, 2010). Despite decreases in emissions of O_3 precursors over Europe since 1990, EEA (2014) reports that 98 % of Europe’s urban population are exposed to levels exceeding the WHO air quality guideline of $100 \mu\text{g m}^{-3}$ over an 8 h mean. These exceedances result from local and regional O_3 precursor gas emissions, their intercontinental transport and the non-linear relationship of O_3 concentrations to NO_x and VOC levels (EEA, 2014).

Effective strategies for emission reductions rely on accurate predictions of O_3 concentrations using chemical transport models (CTMs). These predictions require adequate representation of gas-phase chemistry in the chemical mechanism used by the CTM. For reasons of computational efficiency, the chemical mechanisms used by global and regional CTMs must be simpler than the nearly explicit mechanisms which can be used in box modelling studies. This study compares the impacts of different simplification approaches of chemical mechanisms on O_3 production chemistry focusing on the role of VOC degradation products.



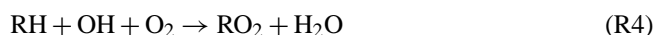
The photochemical cycle (Reactions R1–R3) rapidly produces and destroys O_3 . NO and NO_2 reach a near-steady state via Reactions (R1) and (R2) which is disturbed in two cases. Firstly, via O_3 removal (deposition or Reaction R1 during night-time and near large NO sources) and secondly,

1 Introduction

Ground-level ozone (O_3) is both an air pollutant and a climate forcer that is detrimental to human health and crop growth (Stevenson et al., 2013). O_3 is produced from the reactions of volatile organic compounds (VOCs) and nitro-

when O_3 is produced through VOC– NO_x chemistry (Sillman, 1999).

VOCs (RH) are mainly oxidised in the troposphere by the hydroxyl radical (OH) forming peroxy radicals (RO_2) in the presence of O_2 . For example, Reaction (R4) describes the OH oxidation of alkanes proceeding through abstraction of an H from the alkane. In high- NO_x conditions, typical of urban environments, RO_2 react with NO (Reaction R5) to form alkoxy radicals (RO), which react quickly with O_2 (Reaction R6) producing a hydroperoxy radical (HO_2) and a carbonyl species ($R'CHO$). The secondary chemistry of these first-generation carbon-containing oxidation products is analogous to the sequence of Reactions (R4–R6), producing further HO_2 and RO_2 radicals. Subsequent-generation oxidation products can continue to react, producing HO_2 and RO_2 until they have been completely oxidised to CO_2 and H_2O . Both RO_2 and HO_2 react with NO to produce NO_2 (Reactions R5 and R7) leading to O_3 production via Reactions (R2) and (R3). Thus, the amount of O_3 produced from VOC degradation is related to the number of NO to NO_2 conversions by RO_2 and HO_2 radicals formed during VOC degradation (Atkinson, 2000).

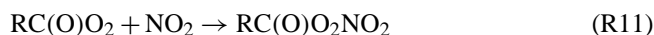


Three atmospheric regimes with respect to O_3 production can be defined (Jenkin and Clemitshaw, 2000). In the NO_x -sensitive regime, VOC concentrations are much higher than those of NO_x , and O_3 production depends on NO_x concentrations. On the other hand, when NO_x concentrations are much higher than those of VOCs (VOC-sensitive regime), VOC concentrations determine the amount of O_3 produced. Finally, the NO_x –VOC-sensitive regime produces maximal O_3 and is controlled by both VOC and NO_x concentrations.

These atmospheric regimes remove radicals through distinct mechanisms (Kleinman, 1991). In the NO_x -sensitive regime, radical concentrations are high relative to NO_x leading to radical removal by radical combination (Reaction R8) and bimolecular destruction (Reaction R9) (Kleinman, 1994).



However, in the VOC-sensitive regime, radicals are removed by reacting with NO_2 leading to nitric acid (HNO_3) (Reaction R10) and PAN species (Reaction R11).



The NO_x –VOC-sensitive regime has no dominant radical removal mechanism as radical and NO_x amounts are compara-

ble. This chemistry results in O_3 concentrations being a non-linear function of NO_x and VOC concentrations.

Individual VOCs impact O_3 production differently through their diverse reaction rates and degradation pathways. These impacts can be quantified using ozone production potentials (OPPs), which can be calculated through incremental reactivity (IR) studies using photochemical models. In IR studies, VOC concentrations are changed by a known increment and the change in O_3 production is compared to that of a standard VOC mixture. Examples of IR scales are the maximum incremental reactivity (MIR) and maximum ozone incremental reactivity (MOIR) scales in Carter (1994), as well as the photochemical ozone creation potential (POCP) scale of Derwent et al. (1996, 1998). The MIR, MOIR and POCP scales were calculated under different NO_x conditions, thus calculating OPPs in different atmospheric regimes.

Butler et al. (2011) calculate the maximum potential of a number of VOCs to produce O_3 by using NO_x conditions inducing NO_x –VOC-sensitive chemistry over multi-day scenarios using a “tagging” approach – the tagged ozone production potential (TOPP). Tagging involves labelling all organic degradation products produced during VOC degradation with the name of the emitted VOCs. Tagging enables the attribution of O_3 production from VOC degradation products back to the emitted VOCs, thus providing detailed insight into VOC degradation chemistry. Butler et al. (2011), using a near-explicit chemical mechanism, showed that some VOCs, such as alkanes, produce maximum O_3 on the second day of the model run; in contrast to unsaturated aliphatic and aromatic VOCs which produce maximum O_3 on the first day. In this study, the tagging approach of Butler et al. (2011) is applied to several chemical mechanisms of reduced complexity, using conditions of maximum O_3 production (NO_x –VOC-sensitive regime), to compare the effects of different representations of VOC degradation chemistry on O_3 production in the different chemical mechanisms.

A near-explicit mechanism, such as the Master Chemical Mechanism (MCM) (Jenkin et al., 2003; Saunders et al., 2003; Bloss et al., 2005), includes detailed degradation chemistry making the MCM ideal as a reference for comparing chemical mechanisms. Reduced mechanisms generally take two approaches to simplifying the representation of VOC degradation chemistry: lumped-structure approaches and lumped-molecule approaches (Dodge, 2000).

Lumped-structure mechanisms speciate VOCs by the carbon bonds of the emitted VOCs (e.g. the Carbon Bond mechanisms, CBM-IV (Gery et al., 1989) and CB05 (Yarwood et al., 2005)). Lumped-molecule mechanisms represent VOCs explicitly or by aggregating (lumping) many VOCs into a single mechanism species. Mechanism species may lump VOCs by functionality (MOdel for Ozone and Related chemical Tracers, MOZART-4, Emmons et al., 2010) or OH reactivity (Regional Acid Deposition Model, RADM2 (Stockwell et al., 1990), Regional Atmospheric Chemistry

Mechanism, RACM (Stockwell et al., 1997) and RACM2 (Goliff et al., 2013)). The Common Representative Intermediates mechanism (CRI) lumps the degradation products of VOCs rather than the emitted VOCs (Jenkin et al., 2008).

Many comparison studies of chemical mechanisms consider modelled time series of O_3 concentrations over varying VOC and NO_x concentrations. Examples are Dunker et al. (1984), Kuhn et al. (1998) and Emmerson and Evans (2009). The largest discrepancies between the time series of O_3 concentrations in different mechanisms from these studies arise when modelling urban rather than rural conditions and are attributed to the treatment of radical production, organic nitrate and night-time chemistry. Emmerson and Evans (2009) also compare the inorganic gas-phase chemistry of different chemical mechanisms; differences in inorganic chemistry arise from inconsistencies between IUPAC and JPL reaction rate constants.

Mechanisms have also been compared using OPP scales. OPPs are a useful comparison tool as they relate O_3 production to a single value. Derwent et al. (2010) compared the near-explicit MCM v3.1 and SAPRC-07 mechanisms using first-day POCP values calculated under VOC-sensitive conditions. The POCP values were comparable between the mechanisms. Butler et al. (2011) compared first-day TOPP values to the corresponding published MIR, MOIR and POCP values. TOPP values were most comparable to MOIR and POCP values due to the similarity of the chemical regimes used in their calculation.

In this study, we compare TOPP values of VOCs using a number of mechanisms to those calculated with the MCM v3.2, under standardised conditions which maximise O_3 production. Differences in O_3 production are explained by the differing treatments of secondary VOC degradation in these mechanisms.

2 Methodology

2.1 Chemical mechanisms

The nine chemical mechanisms compared in this study are outlined in Table 1 with a brief summary below. We used a subset of each chemical mechanism containing all the reactions needed to fully describe the degradation of the VOCs in Table 2. The reduced mechanisms in this study were chosen as they are commonly used in 3-D models and apply different approaches to representing secondary VOC chemistry. The recent review by Baklanov et al. (2014) shows that each chemical mechanism used in this study are actively used by modelling groups.

The MCM (Jenkin et al., 1997, 2003; Saunders et al., 2003; Bloss et al., 2005; Rickard et al., 2015) is a near-explicit mechanism which describes the degradation of 125 primary VOCs. The MCM v3.2 is the reference mechanism in this study due to its level of detail (16 349 organic reac-

tions). Despite this level of detail, the MCM had difficulties in reproducing the results of chamber study experiments involving aromatic VOCs (Bloss et al., 2005).

The CRI (Jenkin et al., 2008) is a reduced chemical mechanism with 1145 organic reactions describing the oxidation of the same primary VOCs as the MCM v3.1 (12 691 organic reactions). VOC degradation in the CRI is simplified by lumping the degradation products of many VOCs into mechanism species whose overall O_3 production reflects that of the MCM v3.1. The CRI v2 is available in more than one reduced variant, described in Watson et al. (2008). We used a subset of the full version of the CRI v2 (<http://mcm.leeds.ac.uk/CRI>). Differences in O_3 production between the CRI v2 and MCM v3.2 may be due to changes in the MCM versions rather than the CRI reduction techniques, hence the MCM v3.1 is also included in this study.

MOZART-4 represents global tropospheric and stratospheric chemistry (Emmons et al., 2010). Explicit species exist for methane, ethane, propane, ethene, propene, isoprene and α -pinene. All other VOCs are represented by lumped species determined by the functionality of the VOCs. Tropospheric chemistry is described by 145 organic reactions in MOZART-4.

RADM2 (Stockwell et al., 1990) describes regional-scale atmospheric chemistry using 145 organic reactions with explicit species representing methane, ethane, ethene and isoprene. All other VOCs are assigned to lumped species based on OH reactivity and molecular weight. RADM2 was updated to RACM (Stockwell et al., 1997) with more explicit and lumped species representing VOCs as well as revised chemistry (193 organic reactions). RACM2 is the updated RACM version (Goliff et al., 2013) with substantial updates to the chemistry, including more lumped and explicit species representing emitted VOCs (315 organic reactions).

CBM-IV (Gery et al., 1989) uses 46 organic reactions to simulate polluted urban conditions and represents ethene, formaldehyde and isoprene explicitly while all other emitted VOCs are lumped by their carbon bond types. All primary VOCs were assigned to lumped species in CBM-IV as described in Hogo and Gery (1989). For example, the mechanism species PAR represents the C–C bond. Pentane, having five carbon atoms, is represented as 5 PAR. A pentane mixing ratio of 1200 pptv is assigned to 6000 ($= 1200 \times 5$) pptv of PAR in CBM-IV. CBM-IV was updated to CB05 (Yarwood et al., 2005) by including further explicit species representing methane, ethane and acetaldehyde, and has 99 organic reactions. Other updates include revised allocation of primary VOCs and updated rate constants.

2.2 Model set-up

The modelling approach and set-up follows the original TOPP study of Butler et al. (2011). The approach is summarised here; further details can be found in the Supplement and in Butler et al. (2011). We use the MECCA box model,

Table 1. The chemical mechanisms used in the study are shown here. MCM v3.2 is the reference mechanism. The number of organic species and reactions needed to fully oxidise the VOCs in Table 2 for each mechanism are also included.

Chemical mechanism	Number of organic species	Number of organic reactions	Type of lumping	Reference	Recent study
MCM v3.2	1884	5621	No lumping	Rickard et al. (2015)	Koss et al. (2015)
MCM v3.1	1677	4862	No lumping	Jenkin et al. (1997)	Lidster et al. (2014)
				Saunders et al. (2003)	
				Jenkin et al. (2003)	
				Bloss et al. (2005)	
CRI v2	189	559	Lumped intermediates	Jenkin et al. (2008)	Derwent et al. (2015)
MOZART-4	61	135	Lumped molecule	Emmons et al. (2010)	Hou et al. (2015)
RADM2	42	105	Lumped molecule	Stockwell et al. (1990)	Li et al. (2014)
RACM	51	152	Lumped molecule	Stockwell et al. (1997)	Ahmadov et al. (2015)
RACM2	92	244	Lumped molecule	Goliff et al. (2013)	Goliff et al. (2015)
CBM-IV	19	47	Lumped structure	Gery et al. (1989)	Foster et al. (2014)
CB05	33	86	Lumped structure	Yarwood et al. (2005)	Dunker et al. (2015)

originally described by Sander et al. (2005), and as subsequently modified by Butler et al. (2011) to include MCM chemistry. In this study, the model is run under conditions representative of 34° N at the equinox (broadly representative of the city of Los Angeles, USA).

Maximum O₃ production is achieved in each model run by balancing the chemical source of radicals and NO_x at each time step by emitting the appropriate amount of NO. These NO_x conditions induce NO_x–VOC-sensitive chemistry. Ambient NO_x conditions are not required as this study calculates the maximum potential of VOCs to produce O₃. Future work should verify the extent to which the maximum potential of VOCs to produce O₃ is reached under ambient NO_x conditions.

VOCs typical of Los Angeles and their initial mixing ratios are taken from Baker et al. (2008), listed in Table 2. Following Butler et al. (2011), the associated emissions required to keep the initial mixing ratios of each VOC constant until noon of the first day were determined for the MCM v3.2. These emissions are subsequently used for each mechanism, ensuring the amount of each VOC emitted was the same in every model run. Methane (CH₄) was fixed at 1.8 ppmv while CO and O₃ were initialised at 200 and 40 ppbv and then allowed to evolve freely.

The VOCs used in this study are assigned to mechanism species following the recommendations from the literature of each mechanism (Table 1), the representation of each VOC in the mechanisms is found in Table 2. Emissions of lumped species are weighted by the carbon number of the mechanism species ensuring the total amount of emitted reactive carbon was the same in each model run.

The MECCA box model is based upon the Kinetic Pre-Processor (KPP) (Damian et al., 2002). Hence, all chemical mechanisms were adapted into modularised KPP format. The inorganic gas-phase chemistry described in the MCM v3.2 was used in each run to remove any differences between

treatments of inorganic chemistry in each mechanism. Thus, differences between the O₃ produced by the mechanisms are due to the treatment of organic degradation chemistry.

The MCM v3.2 approach to photolysis, dry deposition of VOC oxidation intermediates and RO₂–RO₂ reactions was used for each mechanism; details of these adaptations can be found in the Supplement. Some mechanisms include reactions which are only important in the stratosphere or free troposphere. For example, PAN photolysis is only important in the free troposphere (Harwood et al., 2003) and was removed from MOZART-4, RACM2 and CB05 for the purpose of the study, as this study considers processes occurring within the planetary boundary layer.

2.3 Tagged ozone production potential (TOPP)

This section summarises the tagging approach described in Butler et al. (2011) which is applied in this study.

2.3.1 O_x family and tagging approach

O₃ production and loss is dominated by rapid photochemical cycles, such as Reactions (R1)–(R3). The effects of rapid production and loss cycles can be removed by using chemical families that include rapidly inter-converting species. In this study, we define the O_x family to include O₃, O(³P), O(¹D), NO₂ and other species involved in fast cycling with NO₂, such as HO₂NO₂ and PAN species. Thus, production of O_x can be used as a proxy for production of O₃.

The tagging approach follows the degradation of emitted VOCs through all possible pathways by labelling every organic degradation product with the name of the emitted VOCs. Thus, each emitted VOC effectively has its own set of degradation reactions. Butler et al. (2011) showed that O_x production can be attributed to the VOCs by following the tags of each VOC.

Table 2. Non-methane volatile organic compounds (NMVOCs) present in Los Angeles. Mixing ratios are taken from Baker et al. (2008) and their representation in each chemical mechanism. The representation of the VOCs in each mechanism is based upon the recommendations of the literature for each mechanism (Table 1).

NMVOCs	Mixing ratio (pptv)	MCM v3.1, v3.2, CRI v2	MOZART-4	RADM2	RACM	RACM2	CBM-IV	CB05
Alkanes								
Ethane	6610	C2H6	C2H6	ETH	ETH	ETH	0.4 PAR	ETHA
Propane	6050	C3H8	C3H8	HC3	HC3	HC3	1.5 PAR	1.5 PAR
Butane	2340	NC4H10	BIGALK	HC3	HC3	HC3	4 PAR	4 PAR
2-Methylpropane	1240	IC4H10	BIGALK	HC3	HC3	HC3	4 PAR	4 PAR
Pentane	1200	NC5H12	BIGALK	HC5	HC5	HC5	5 PAR	5 PAR
2-Methylbutane	2790	IC5H12	BIGALK	HC5	HC5	HC5	5 PAR	5 PAR
Hexane	390	NC6H14	BIGALK	HC5	HC5	HC5	6 PAR	6 PAR
Heptane	160	NC7H16	BIGALK	HC5	HC5	HC5	7 PAR	7 PAR
Octane	80	NC8H18	BIGALK	HC8	HC8	HC8	8 PAR	8 PAR
Alkenes								
Ethene	2430	C2H4	C2H4	OL2	ETE	ETE	ETH	ETH
Propene	490	C3H6	C3H6	OLT	OLT	OLT	OLE + PAR	OLE + PAR
Butene	65	BUT1ENE	BIGENE	OLT	OLT	OLT	OLE + 2 PAR	OLE + 2 PAR
2-Methylpropene	130	MEPROPENE	BIGENE	OLI	OLI	OLI	PAR + FORM + ALD2	FORM + 3 PAR
Isoprene	270	C5H8	ISOP	ISO	ISO	ISO	ISOP	ISOP
Aromatics								
Benzene	480	BENZENE	TOLUENE	TOL	TOL	BEN	PAR	PAR
Toluene	1380	TOLUENE	TOLUENE	TOL	TOL	TOL	TOL	TOL
m-Xylene	410	MXYL	TOLUENE	XYL	XYL	XYM	XYL	XYL
p-Xylene	210	PXYL	TOLUENE	XYL	XYL	XYP	XYL	XYL
o-Xylene	200	OXYL	TOLUENE	XYL	XYL	XYO	XYL	XYL
Ethylbenzene	210	EBENZ	TOLUENE	TOL	TOL	TOL	TOL + PAR	TOL + PAR

O_x production from lumped-mechanism species are re-assigned to the VOCs of Table 2 by scaling the O_x production of the mechanism species by the fractional contribution of each represented VOC. For example, TOL in RACM2 represents toluene and ethylbenzene with fractional contributions of 0.87 and 0.13 to TOL emissions. Scaling the O_x production from TOL by these factors gives the O_x production from toluene and ethylbenzene in RACM2.

Many reduced mechanisms use an operator species as a surrogate for RO_2 during VOC degradation enabling these mechanisms to produce O_x while minimising the number of RO_2 species represented. O_x production from operator species is assigned as O_x production from the organic degradation species producing the operator. This allocation technique is also used to assign O_x production from HO_2 via Reaction (R7).

2.3.2 Definition of TOPP

Attributing O_x production to individual VOCs using the tagging approach is the basis for calculating the TOPP of a VOC, which is defined as the number of O_x molecules produced per emitted molecule of VOC. The TOPP value of

a VOC that is not represented explicitly in a chemical mechanism is calculated by multiplying the TOPP value of the mechanism species representing the VOCs by the ratio of the carbon numbers of the VOCs to the mechanism species. For example, CB05 represents hexane as 6 PAR, so the TOPP value of hexane in the CB05 is 6 times the TOPP of PAR. MOZART-4 represents hexane with the five carbon species BIGALK. Thus, hexane emissions are represented molecule for molecule as $\frac{6}{5}$ of the equivalent number of molecules of BIGALK, and the TOPP value of hexane in MOZART-4 is calculated by multiplying the TOPP value of BIGALK by $\frac{6}{5}$.

3 Results

3.1 Ozone time series and O_x production budgets

Figure 1 shows the time series of O_3 mixing ratios obtained with each mechanism. There is an 8 ppbv difference in O_3 mixing ratios on the first day between RADM2, which has the highest O_3 , and RACM2, which has the lowest O_3 mixing ratios when not considering the outlier time series of RACM. The difference between RADM2 and RACM, the low outlier, was 21 ppbv on the first day. The O_3 mixing ratios in

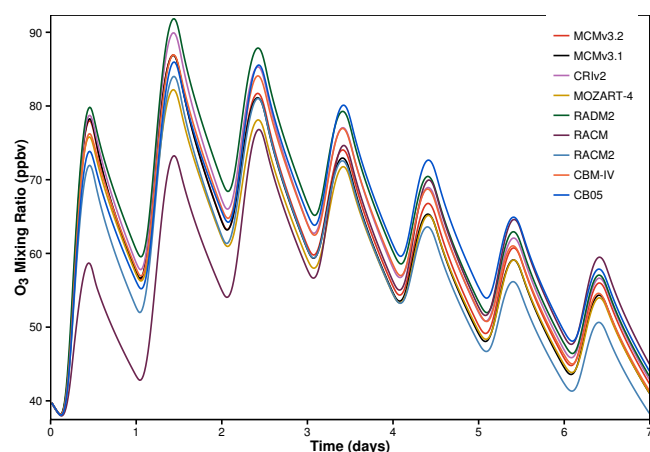


Figure 1. Time series of O_3 mixing ratios obtained using each mechanism.

the CRI v2 are larger than those in the MCM v3.1, which is similar to the results in Jenkin et al. (2008) where the O_3 mixing ratios of the CRI v2 and MCM v3.1 are compared over a 5-day period.

The O_3 mixing ratios in Fig. 1 are influenced by the approaches used in developing the chemical mechanisms and not a function of the explicitness of the chemical mechanism. For example, the O_3 mixing ratios obtained using the Carbon Bond mechanisms (CBM-IV and CB05) compare well with the MCM despite both Carbon Bond mechanisms having $\sim 1\%$ of the number of reactions in the MCM v3.2. Also, the O_3 mixing ratios from RACM2 and RADM2 show similar absolute differences from that of the MCM despite RACM2 having more than double the number of reactions of RADM2.

The day-time O_x production budgets allocated to individual VOCs for each mechanism are shown in Fig. 2. The relationships between O_3 mixing ratios in Fig. 1 are mirrored in Fig. 2 where mechanisms producing high amounts of O_x also have high O_3 mixing ratios. The conditions in the box model lead to a daily maximum of OH that increases with each day leading to an increase on each day in both the reaction rate of the OH oxidation of CH_4 and the daily contribution of CH_4 to O_x production.

The first-day mixing ratios of O_3 in RACM are lower than other mechanisms due to a lack of O_x production from aromatic VOCs on the first day in RACM (Fig. 2). Aromatic degradation chemistry in RACM results in net loss of O_x on the first day, described later in Sect. 3.2.1.

RADM2 is the only reduced mechanism that produces higher O_3 mixing ratios than the more detailed mechanisms (MCM v3.2, MCM v3.1 and CRI v2). Higher mixing ratios of O_3 in RADM2 are produced due to increased O_x production from propane compared to the MCM v3.2; on the first day, the O_x production from propane in RADM2 is triple that of the MCM v3.2 (Fig. 2). Propane is represented as HC3 in

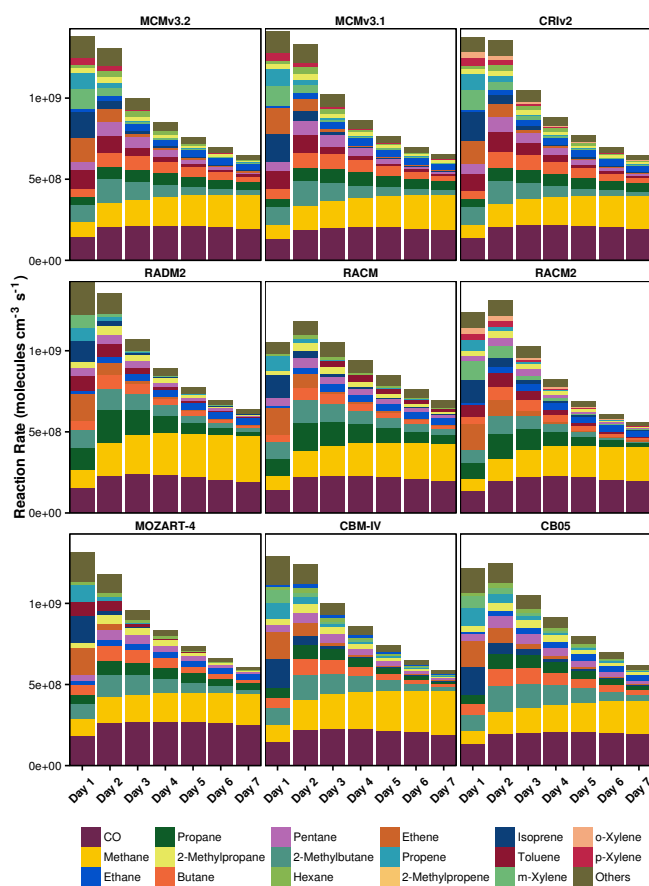


Figure 2. Day-time O_x production budgets in each mechanism allocated to individual VOCs.

RADM2 (Stockwell et al., 1990) and the degradation of HC3 has a lower yield of the less-reactive ketones compared to the MCM. The further degradation of ketones hinders O_x production due to the low OH reactivity and photolysis rate of ketones. Secondary degradation of HC3 proceeds through the degradation of acetaldehyde (CH_3CHO) propagating O_x production through the reactions of CH_3CO_3 and CH_3O_2 with NO. Thus, the lower ketone yields lead to increased O_x production from propane degradation in RADM2 compared to the MCM v3.2.

3.2 Time-dependent O_x production

Time series of daily TOPP values for each VOC are presented in Fig. 3 and the cumulative TOPP values at the end of the model run obtained for each VOC using each of the mechanisms, normalised by the number of atoms of C in each VOC are presented in Table 3. In the MCM and CRI v2, the cumulative TOPP values obtained for each VOC show that by the end of the model run, larger alkanes have produced more O_x per unit of reactive C than alkenes or aromatic VOCs. By the end of the runs using the lumped-structure mechanisms (CBM-IV and CB05), alkanes produce similar

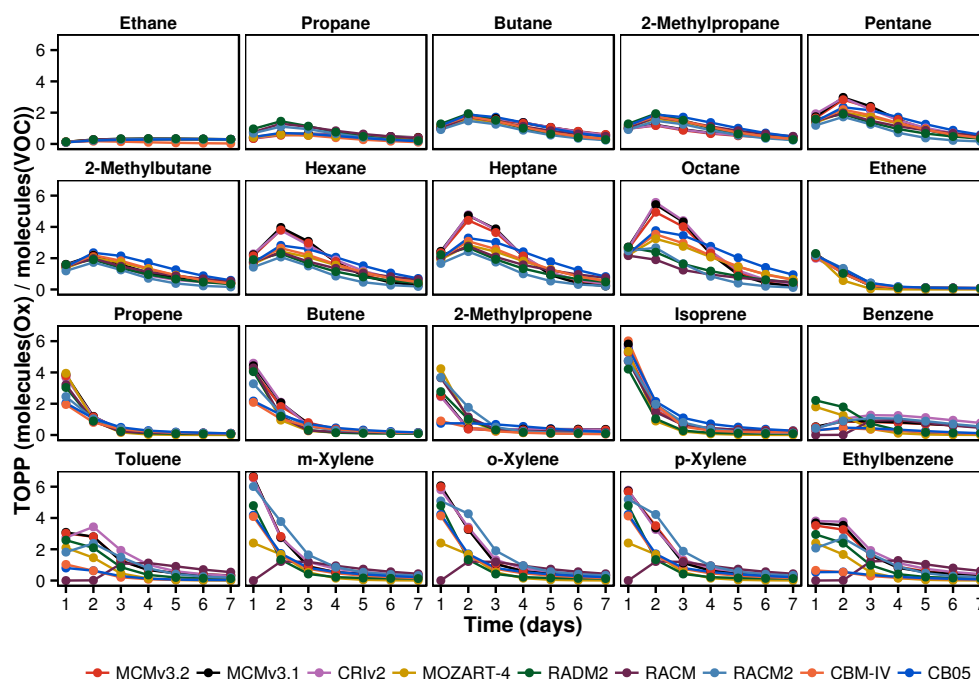


Figure 3. TOPP value time series using each mechanism for each VOC.

Table 3. Cumulative TOPP values at the end of the model run for all VOCs with each mechanism, normalised by the number of C atoms in each VOC.

NMVOCS	MCM v3.2	MCM v3.1	CRI v2	MOZART-4	RADM2	RACM	RACM2	CBM-IV	CB05
Alkanes									
Ethane	0.9	1.0	0.9	0.9	1.0	1.0	0.9	0.3	0.9
Propane	1.1	1.2	1.2	1.1	1.8	1.8	1.4	0.9	1.0
Butane	2.0	2.0	2.0	1.7	1.8	1.8	1.4	1.7	2.1
2-Methylpropane	1.3	1.3	1.3	1.7	1.8	1.8	1.4	1.7	2.1
Pentane	2.1	2.1	2.2	1.7	1.5	1.6	1.1	1.7	2.1
2-Methylbutane	1.6	1.6	1.5	1.7	1.5	1.6	1.1	1.7	2.1
Hexane	2.1	2.1	2.2	1.7	1.5	1.6	1.1	1.7	2.1
Heptane	2.0	2.1	2.2	1.7	1.5	1.6	1.1	1.7	2.1
Octane	2.0	2.0	2.2	1.7	1.2	1.0	1.0	1.7	2.1
Alkenes									
Ethene	1.9	1.9	1.9	1.4	2.0	2.0	2.2	1.9	2.2
Propene	1.9	2.0	1.9	1.7	1.5	1.6	1.5	1.2	1.4
Butene	1.9	2.0	2.0	1.5	1.5	1.6	1.5	0.8	0.9
2-Methylpropene	1.1	1.2	1.2	1.5	1.1	1.5	1.6	0.5	0.5
Isoprene	1.8	1.8	1.8	1.3	1.2	1.6	1.7	1.9	2.1
Aromatics									
Benzene	0.8	0.8	1.1	0.6	0.9	0.6	0.9	0.3	0.3
Toluene	1.3	1.3	1.5	0.6	0.9	0.6	1.0	0.3	0.3
m-Xylene	1.5	1.5	1.6	0.6	0.9	0.6	1.7	0.9	1.0
p-Xylene	1.5	1.5	1.6	0.6	0.9	0.6	1.7	0.9	1.0
o-Xylene	1.5	1.5	1.6	0.6	0.9	0.6	1.7	0.9	1.0
Ethylbenzene	1.3	1.4	1.5	0.6	0.9	0.6	1.0	0.2	0.3

amounts of O_x per reactive C, while aromatic VOCs and some alkenes produce less O_x per reactive C than the MCM. However, in lumped-molecule mechanisms (MOZART-4, RADM2, RACM, RACM2), practically all VOCs produce less O_x per reactive C than the MCM by the end of the run. This lower efficiency of O_x production from many individual VOCs in lumped-molecule and lumped-structure mechanisms would lead to an underestimation of O_3 levels downwind of an emission source, and a smaller contribution to background O_3 when using lumped-molecule and lumped-structure mechanisms.

The lumped-intermediate mechanism (CRI v2) produces the most similar O_x to the MCM v3.2 for each VOC, seen in Fig. 3 and Table 3. Higher variability in the time-dependent O_x production is evident for VOCs represented by lumped-mechanism species. For example, 2-methylpropene, represented in the reduced mechanisms by a variety of lumped species, has a higher spread in time-dependent O_x production than ethene, which is explicitly represented in each mechanism.

In general, the largest differences in O_x produced by aromatic and alkene species are on the first day of the simulations, while the largest inter-mechanism differences in O_x produced by alkanes are on the second and third days of the simulations. The reasons for these differences in behaviour will be explored in Sect. 3.2.1, which examines differences in first day O_x production between the chemical mechanisms, and Sect. 3.2.2, which examines the differences in O_x production on subsequent days.

3.2.1 First-day ozone production

The first-day TOPP values of each VOC from each mechanism, representing O_3 production from freshly emitted VOCs near their source region, are compared to those obtained with the MCM v3.2 in Fig. 4. The root mean square error (RMSE) of all first-day TOPP values in each mechanism relative to those in the MCM v3.2 are also included in Fig. 4. The RMSE value of the CRI v2 shows that first-day O_x production from practically all the individual VOC matches that in the MCM v3.2. All other reduced mechanisms have much larger RMSE values indicating that the first-day O_x production from the majority of the VOCs differs from that in the MCM v3.2.

The reduced complexity of reduced mechanisms means that aromatic VOCs are typically represented by one or two mechanism species leading to differences in O_x production of the actual VOCs compared to the MCM v3.2. For example, all aromatic VOCs in MOZART-4 are represented as toluene, thus less-reactive aromatic VOCs, such as benzene, produce higher O_x whilst more-reactive aromatic VOCs, such as the xylenes, produce less O_x in MOZART-4 than the MCM v3.2. RACM2 includes explicit species representing benzene, toluene and each xylene resulting in O_x production

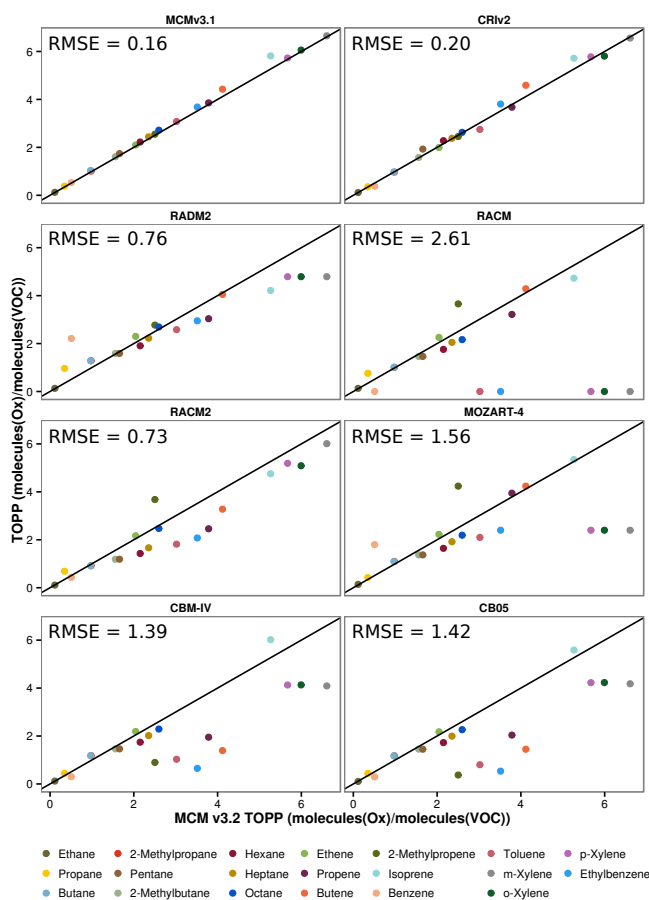


Figure 4. The first-day TOPP values for each VOC calculated using MCM v3.2 and the corresponding values in each mechanism. The root mean square error (RMSE) of each set of TOPP values is also displayed. The black line is the 1 : 1 line.

that is the most similar to the MCM v3.2 than other reduced mechanisms.

Figure 3 shows a high spread in O_x production from aromatic VOCs on the first day indicating that aromatic degradation is treated differently between mechanisms. Toluene degradation is examined in more detail by comparing the reactions contributing to O_x production and loss in each mechanism, shown in Fig. 5. These reactions are determined by following the “toluene” tags in the tagged version of each mechanism.

Toluene degradation in RACM includes several reactions consuming O_x that are not present in the MCM, resulting in net loss of O_x on the first 2 days. Ozonolysis of the cresol OH adduct mechanism species, ADDC, contributes significantly to O_x loss in RACM. This reaction was included in RACM due to improved cresol product yields when comparing RACM predictions with experimental data (Stockwell et al., 1997). Other mechanisms that include cresol OH adduct species do not include ozonolysis and these reactions are not included in the updated RACM2.

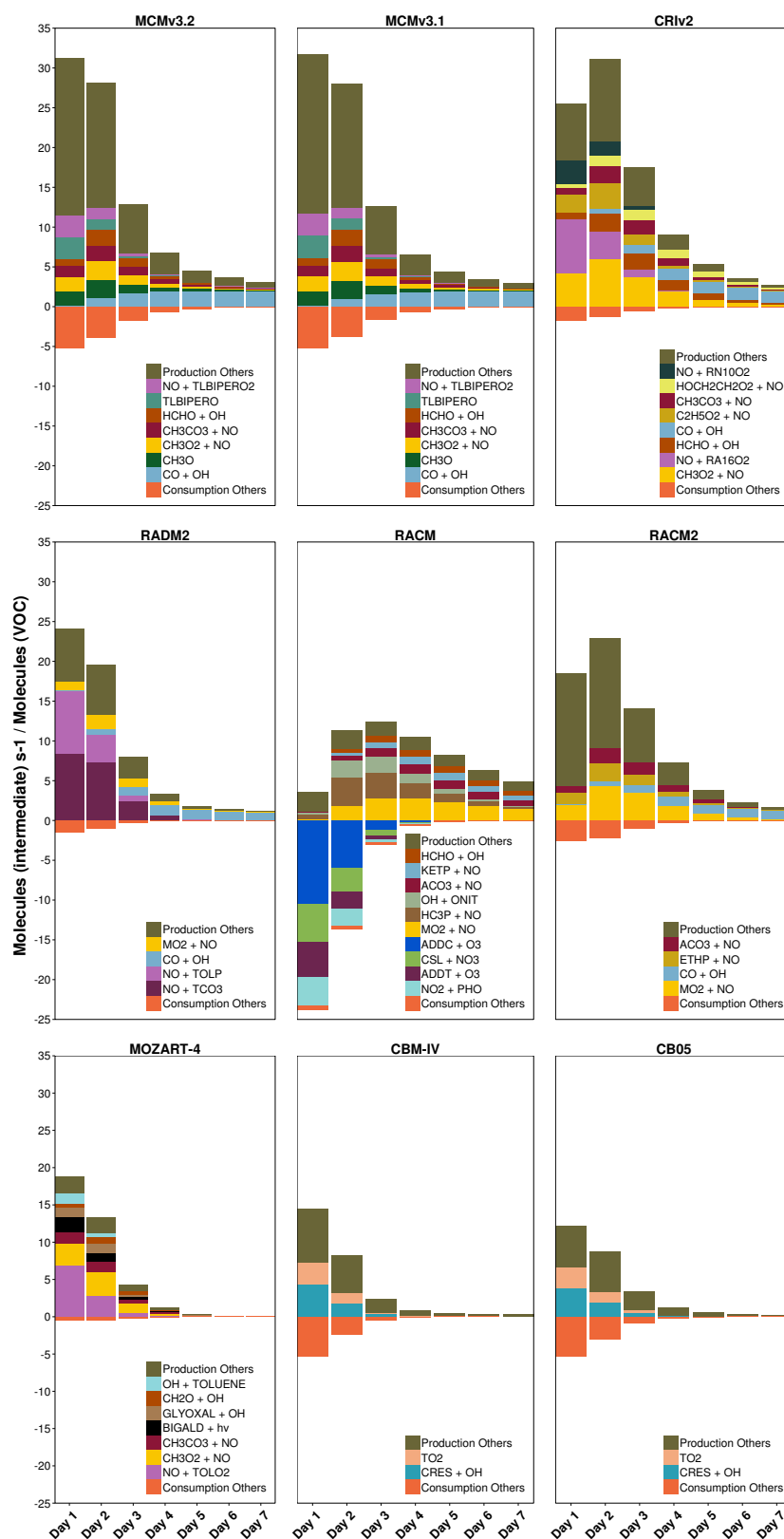


Figure 5. Day-time O_x production and loss budgets allocated to the responsible reactions during toluene degradation in all mechanisms. These reactions are presented using the species defined in each mechanism in Table 1.

The total O_x produced on the first day during toluene degradation in each reduced mechanism is less than that in the MCM v3.2 (Fig. 5). Less O_x is produced in all reduced mechanisms due to a faster breakdown of the VOCs into smaller fragments than the MCM, described later in Sect. 3.3. Moreover, in CBM-IV and CB05, less O_x is produced during toluene degradation as reactions of the toluene degradation products CH_3O_2 and CO do not contribute to the O_x production budgets, which is not the case in any other mechanism (Fig. 5).

Maximum O_x production from toluene degradation in CRI v2 and RACM2 is reached on the second day in contrast to the MCM v3.2 which produces peak O_x on the first day. The second-day maximum of O_x production in CRI v2 and RACM2 from toluene degradation results from more efficient production of unsaturated dicarbonyls than the MCM v3.2. The degradation of unsaturated dicarbonyls produces peroxy radicals such as $C_2H_5O_2$ which promote O_x production via reactions with NO.

Unsaturated aliphatic VOCs generally produce similar amounts of O_x between mechanisms, especially explicitly represented VOCs, such as ethene and isoprene. On the other hand, unsaturated aliphatic VOCs that are not explicitly represented produce differing amounts of O_x between mechanisms (Fig. 3). For example, the O_x produced during 2-methylpropene degradation varies between mechanisms; differing rate constants of initial oxidation reactions and non-realistic secondary chemistry lead to these differences; further details are found in the Supplement.

Non-explicit representations of aromatic and unsaturated aliphatic VOCs coupled with differing degradation chemistry and a faster breakdown into smaller-size degradation products results in different O_x production in lumped-molecule and lumped-structure mechanisms compared to the MCM v3.2.

3.2.2 Ozone production on subsequent days

Alkane degradation in CRI v2 and both MCMs produces a second-day maximum in O_x that increases with alkane carbon number (Fig. 3). The increase in O_x production on the second day is reproduced for each alkane by the reduced mechanisms, except octane in RADM2, RACM and RACM2. However, larger alkanes produce less O_x than the MCM on the second day in all lumped-molecule and lumped-structure mechanisms.

The lumped-molecule mechanisms (MOZART-4, RADM2, RACM and RACM2) represent many alkanes by mechanism species which may lead to unrepresentative secondary chemistry for alkane degradation. For example, 3 times more O_x is produced during the degradation of propane in RADM2 than the MCM v3.2 on the first day (Fig. 2). Propane is represented in RADM2 by the mechanism species HC3 which also represents other classes of VOCs, such as alcohols. The secondary chemistry of HC3 is

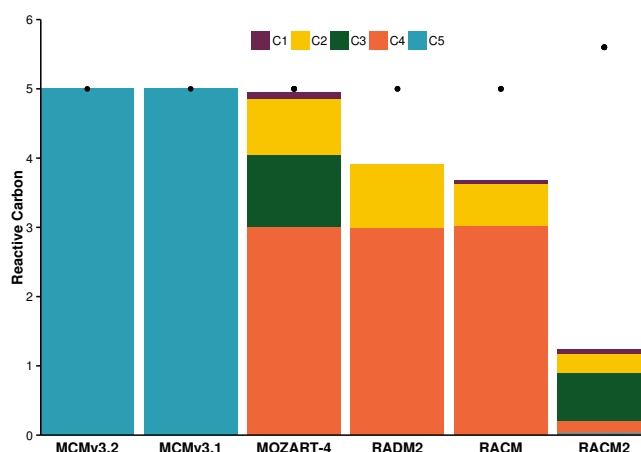


Figure 6. The distribution of reactive carbon in the products of the reaction between NO and the pentyl peroxy radical in lumped-molecule mechanisms compared to the MCM. The black dot represents the reactive carbon of the pentyl peroxy radical.

tailored to produce O_x from these different VOCs and differs from alkane degradation in the MCM v3.2 by producing less ketones in RADM2.

As will be shown in Sect. 3.3, another feature of reduced mechanisms is that the breakdown of emitted VOCs into smaller-sized degradation products is faster than the MCM. Alkanes are broken down quicker in CBM-IV, CB05, RADM2, RACM and RACM2 through a higher rate of reactive carbon loss than the MCM v3.2 (shown for pentane and octane in Fig. 8); reactive carbon is lost through reactions not conserving carbon. Despite many degradation reactions of alkanes in MOZART-4 almost conserving carbon, the organic products have less reactive carbon than the organic reactant also speeding up the breakdown of the alkane compared to the MCM v3.2.

For example, Fig. 6 shows the distribution of reactive carbon in the reactants and products from the reaction of NO with the pentyl peroxy radical in both MCMs and each lumped-molecule mechanism. In all the lumped-molecule mechanisms, the individual organic products have less reactive carbon than the organic reactant. Moreover, in RADM2, RACM and RACM2, this reaction does not conserve reactive carbon leading to faster loss rates of reactive carbon.

The faster breakdown of alkanes in lumped-molecule and lumped-structure mechanisms on the first day limits the amount of O_x produced on the second day, as less of the larger-sized degradation products are available for further degradation and O_x production.

3.3 Treatment of degradation products

The time-dependent O_x production of the different VOCs in Fig. 3 results from the varying rates at which VOCs break up into smaller fragments (Butler et al., 2011). Varying breakdown rates of the same VOCs between mechanisms could



Figure 7. Day-time O_x production during pentane and toluene degradation is attributed to the number of carbon atoms of the degradation products for each mechanism.

explain the different time-dependent O_x production between mechanisms. The breakdown of pentane and toluene between mechanisms is compared in Fig. 7 by allocating the O_x production to the number of carbon atoms in the degradation products responsible for O_x production on each day of the model run in each mechanism. Some mechanism species in RADM2, RACM and RACM2 have fractional carbon numbers (Stockwell et al., 1990, 1997; Goliff et al., 2013) and O_x production from these species was reassigned as O_x production of the nearest integral carbon number.

The degradation of pentane, a five-carbon VOC, on the first day in the MCM v3.2 produces up to 50 % more O_x from degradation products also having five carbon atoms than any reduced mechanism. Moreover, the contribution of the degradation products having five carbon atoms in the MCM v3.2 is consistently higher throughout the model run than in re-

duced mechanisms (Fig. 7). Despite producing less total O_x , reduced mechanisms produce up to double the amount of O_x from degradation products with one carbon atom than in the MCM v3.2. The lower contribution of larger degradation products indicates that pentane is generally broken down faster in reduced mechanisms, consistent with the specific example shown for the breakdown of the pentyl peroxy radical in Fig. 6.

The rate of change in reactive carbon during pentane, octane and toluene degradation was determined by multiplying the rate of each reaction occurring during pentane, octane and toluene degradation by its net change in carbon, shown in Fig. 8. Pentane is broken down faster in CBM-IV, CB05, RADM2, RACM and RACM2 by losing reactive carbon more quickly than the MCM v3.2. MOZART-4 also breaks pentane down into smaller-sized products quicker



Figure 8. Daily rate of change in reactive carbon during pentane, octane and toluene degradation. Octane is represented by the five carbon species, BIGALK, in MOZART-4.

than the MCM v3.2 as reactions during pentane degradation in MOZART-4 have organic products whose carbon number is less than the organic reactant, described in Sect. 3.2.2. The faster breakdown of pentane on the first day limits the amount of reactive carbon available to produce further O_x on subsequent days leading to lower O_x production after the first day in reduced mechanisms.

Figure 3 showed that octane degradation produces peak O_x on the first day in RADM2, RACM and RACM2 in contrast to all other mechanisms where peak O_x is produced on the second day. Octane degradation in RADM2, RACM and RACM2 loses reactive carbon much faster than any other mechanism on the first day so that there are not enough degradation products available to produce peak O_x on the second day (Fig. 8). This loss of reactive carbon during alkane degradation leads to the lower accumulated ozone production from these VOCs shown in Table 3.

As seen in Fig. 3, O_x produced during toluene degradation has a high spread between the mechanisms. Figure 7 shows differing distributions of the sizes of the degradation products that produce O_x . All reduced mechanisms omit O_x production from at least one degradation fragment size which produces O_x in the MCM v3.2, indicating that toluene is also broken down more quickly in the reduced mechanisms than the more explicit mechanisms. For example, toluene degradation in RACM2 does not produce O_x from degradation products with six carbons, as is the case in the MCM v3.2. Figure 8 shows that all reduced mechanisms lose reactive carbon during toluene degradation faster than the MCM v3.2. Thus, the degradation of aromatic VOCs in reduced mechanisms are unable to produce similar amounts of O_x as the explicit mechanisms.

4 Conclusions

Tagged ozone production potentials (TOPPs) were used to compare O_x production during VOC degradation in reduced chemical mechanisms to the near-explicit MCM v3.2. First-day mixing ratios of O_3 are similar to the MCM v3.2 for most mechanisms; the O_3 mixing ratios in RACM were much lower than the MCM v3.2 due to a lack of O_x production from the degradation of aromatic VOCs. Thus, RACM may not be the appropriate chemical mechanism when simulating atmospheric conditions having a large fraction of aromatic VOCs.

The lumped-intermediate mechanism, CRI v2, produces the most similar amounts of O_x to the MCM v3.2 for each VOC. The largest differences between O_x production in CRI v2 and MCM v3.2 were obtained for aromatic VOCs; however, overall these differences were much lower than any other reduced mechanism. Thus, when developing chemical mechanisms, the technique of using lumped-intermediate species whose degradation are based upon more detailed mechanism should be considered.

Many VOCs are broken down into smaller-sized degradation products faster on the first day in reduced mechanisms than the MCM v3.2 leading to lower amounts of larger-sized degradation products that can further degrade and produce O_x . Thus, many VOCs in reduced mechanisms produce a lower maximum of O_x and lower total O_x per reactive C by the end of the run than the MCM v3.2. This lower O_x production from many VOCs in reduced mechanisms leads to lower O_3 mixing ratios compared to the MCM v3.2.

Alkanes produce maximum O_3 on the second day of simulations and this maximum is lower in reduced mechanisms than the MCM v3.2 due to the faster breakdown of alkanes into smaller-sized degradation products on the first day. The lower maximum in O_3 production during alkane degradation in reduced mechanisms leads to an underestimation of the O_3 levels downwind of VOC emissions and an underestimation of the VOC contribution to tropospheric background O_3 when using reduced mechanisms in regional or global modelling studies.

This study has determined the maximum potential of VOCs represented in reduced mechanisms to produce O_3 ; this potential may not be reached as ambient NO_x conditions may not induce NO_x –VOC-sensitive chemistry. Moreover, the maximum potential of VOCs to produce O_3 may not be reached when using these reduced mechanisms in 3-D models due to the influence of additional processes, such as mixing and meteorology. Future work shall examine the extent to which the maximum potential of VOCs to produce O_3 in reduced chemical mechanisms is reached using ambient NO_x conditions and including processes found in 3-D models.

The Supplement related to this article is available online at [doi:10.5194/acp-15-8795-2015-supplement](https://doi.org/10.5194/acp-15-8795-2015-supplement).

Acknowledgements. The authors would like to thank Mike Jenkin and William Stockwell for their helpful reviews, as well as Mark Lawrence and Peter J. H. Builtjes for valuable discussions during the preparation of this manuscript.

Edited by: R. Harley

References

- Ahmadov, R., McKeen, S., Trainer, M., Banta, R., Brewer, A., Brown, S., Edwards, P. M., de Gouw, J. A., Frost, G. J., Gilman, J., Helmig, D., Johnson, B., Karion, A., Koss, A., Langford, A., Lerner, B., Olson, J., Oltmans, S., Peischl, J., Pétron, G., Pichugina, Y., Roberts, J. M., Ryerson, T., Schnell, R., Senff, C., Sweeney, C., Thompson, C., Veres, P. R., Warneke, C., Wild, R., Williams, E. J., Yuan, B., and Zamora, R.: Understanding high wintertime ozone pollution events in an oil- and natural gas-producing region of the western US, *Atmos. Chem. Phys.*, 15, 411–429, doi:10.5194/acp-15-411-2015, 2015.
- Atkinson, R.: Atmospheric chemistry of VOCs and NO_x, *Atmos. Environ.*, 34, 2063–2101, 2000.
- Baker, A. K., Beyersdorf, A. J., Doezema, L. A., Katzenstein, A., Meinardi, S., Simpson, I. J., Blake, D. R., and Rowland, F. S.: Measurements of nonmethane hydrocarbons in 28 United States cities, *Atmos. Environ.*, 42, 170–182, 2008.
- Baklanov, A., Schlünzen, K., Suppan, P., Baldasano, J., Brunner, D., Aksoyoglu, S., Carmichael, G., Douros, J., Flemming, J., Forkel, R., Galmarini, S., Gauss, M., Grell, G., Hirtl, M., Joffre, S., Jorba, O., Kaas, E., Kaasik, M., Kallos, G., Kong, X., Korsholm, U., Kurganskiy, A., Kushta, J., Lohmann, U., Mahura, A., Manders-Groot, A., Maurizi, A., Moussiopoulos, N., Rao, S. T., Savage, N., Seigneur, C., Sokhi, R. S., Solazzo, E., Solomos, S., Sørensen, B., Tsegas, G., Vignati, E., Vogel, B., and Zhang, Y.: Online coupled regional meteorology chemistry models in Europe: current status and prospects, *Atmos. Chem. Phys.*, 14, 317–398, doi:10.5194/acp-14-317-2014, 2014.
- Bloss, C., Wagner, V., Jenkin, M. E., Volkamer, R., Bloss, W. J., Lee, J. D., Heard, D. E., Wirtz, K., Martin-Reviejo, M., Rea, G., Wenger, J. C., and Pilling, M. J.: Development of a detailed chemical mechanism (MCMv3.1) for the atmospheric oxidation of aromatic hydrocarbons, *Atmos. Chem. Phys.*, 5, 641–664, doi:10.5194/acp-5-641-2005, 2005.
- Butler, T. M., Lawrence, M. G., Taraborrelli, D., and Lelieveld, J.: Multi-day ozone production potential of volatile organic compounds calculated with a tagging approach, *Atmos. Environ.*, 45, 4082–4090, 2011.
- Carter, W. P. L.: Development of ozone reactivity scales for volatile organic compounds, *J. Air Waste Manage.*, 44, 881–899, 1994.
- Damian, V., Sandu, A., Damian, M., Potra, F., and Carmichael, G.: The kinetic preprocessor KPP – a software environment for solving chemical kinetics, *Comput. Chem. Eng.*, 26, 1567–1579, 2002.
- Derwent, R. G., Jenkin, M. E., and Saunders, S. M.: Photochemical ozone creation potentials for a large number of reactive hydrocarbons under European conditions, *Atmos. Environ.*, 30, 181–199, 1996.
- Derwent, R. G., Jenkin, M. E., Saunders, S. M., and Pilling, M. J.: Photochemical ozone creation potentials for organic compounds in Northwest Europe calculated with a master chemical mechanism, *Atmos. Environ.*, 32, 2429–2441, 1998.
- Derwent, R. G., Jenkin, M. E., Pilling, M. J., Carter, W. P. L., and Kaduwela, A.: Reactivity scales as comparative tools for chemical mechanisms, *J. Air Waste Manage.*, 60, 914–924, 2010.
- Derwent, R. G., Utember, S. R., Jenkin, M. E., and Shallcross, D. E.: Tropospheric ozone production regions and the intercontinental origins of surface ozone over Europe, *Atmos. Environ.*, 112, 216–224, 2015.
- Dodge, M.: Chemical oxidant mechanisms for air quality modeling: critical review, *Atmos. Environ.*, 34, 2103–2130, 2000.
- Dunker, A. M., Kumar, S., and Berzins, P. H.: A comparison of chemical mechanisms used in atmospheric models, *Atmos. Environ.*, 18, 311–321, 1984.
- Dunker, A. M., Koo, B., and Yarwood, G.: Source Apportionment of the Anthropogenic Increment to Ozone, Formaldehyde, and Nitrogen Dioxide by the Path- Integral Method in a 3D Model, *Environ. Sci. Technol.*, 49, 6751–6759, 2015.
- EEA: Air quality in Europe – 2014 report, Tech. Rep. 5/2014, European Environmental Agency, Publications Office of the European Union, doi:10.2800/22847, 2014.
- Emmerson, K. M. and Evans, M. J.: Comparison of tropospheric gas-phase chemistry schemes for use within global models, *Atmos. Chem. Phys.*, 9, 1831–1845, doi:10.5194/acp-9-1831-2009, 2009.
- Emmons, L. K., Walters, S., Hess, P. G., Lamarque, J.-F., Pfister, G. G., Fillmore, D., Granier, C., Guenther, A., Kinnison, D., Laepple, T., Orlando, J., Tie, X., Tyndall, G., Wiedinmyer, C., Baughcum, S. L., and Kloster, S.: Description and evaluation of the Model for Ozone and Related chemical Tracers, version 4 (MOZART-4), *Geosci. Model Dev.*, 3, 43–67, doi:10.5194/gmd-3-43-2010, 2010.
- Foster, P. N., Prentice, I. C., Morfopoulos, C., Siddall, M., and van Weele, M.: Isoprene emissions track the seasonal cycle of canopy temperature, not primary production: evidence from remote sensing, *Biogeosciences*, 11, 3437–3451, doi:10.5194/bg-11-3437-2014, 2014.
- Gery, M. W., Whitten, G. Z., Killus, J. P., and Dodge, M. C.: A photochemical kinetics mechanism for urban and regional scale computer modeling, *J. Geophys. Res.*, 94, 12925–12956, 1989.
- Goliff, W. S., Stockwell, W. R., and Lawson, C. V.: The regional atmospheric chemistry mechanism, version 2, *Atmos. Environ.*, 68, 174–185, 2013.
- Goliff, W. S., Luria, M., Blake, D. R., Zielinska, B., Hallar, G., Valente, R. J., Lawson, C. V., and Stockwell, W. R.: Nighttime air quality under desert conditions, *Atmos. Environ.*, 114, 102–111, 2015.
- Harwood, M., Roberts, J., Frost, G., Ravishankara, A., and Burkholder, J.: Photochemical studies of CH₃C(O)OONO₂ (PAN) and CH₃CH₂C(O)OONO₂ (PPN): NO₃ quantum yields, *J. Phys. Chem. A*, 107, 1148–1154, 2003.
- Hogo, H. and Gery, M.: User's guide for executing OZIPM-4 (Ozone Isopleth Plotting with Optional Mechanisms, Version 4) with CBM-IV (Carbon-Bond Mechanisms-IV) or optional mechanisms. Volume 1. Description of the ozone isopleth plotting package. Version 4, Tech. rep., US Environmental Protection Agency, Durham, North Carolina, USA, 1989.
- Hou, X., Zhu, B., Fei, D., and Wang, D.: The impacts of summer monsoons on the ozone budget of the atmospheric boundary

- layer of the Asia-Pacific region, *Sci. Total Environ.*, 502, 641–649, 2015.
- HTAP: Hemispheric Transport of Air Pollution 2010, Part A: Ozone and Particulate Matter, Air Pollution Studies No.17, Geneva, Switzerland, 2010.
- Jenkin, M. E. and Clemitshaw, K. C.: Ozone and other secondary photochemical pollutants: chemical processes governing their formation in the planetary boundary layer, *Atmos. Environ.*, 34, 2499–2527, 2000.
- Jenkin, M. E., Saunders, S. M., and Pilling, M. J.: The tropospheric degradation of volatile organic compounds: a protocol for mechanism development, *Atmos. Environ.*, 31, 81–104, 1997.
- Jenkin, M. E., Saunders, S. M., Wagner, V., and Pilling, M. J.: Protocol for the development of the Master Chemical Mechanism, MCM v3 (Part B): tropospheric degradation of aromatic volatile organic compounds, *Atmos. Chem. Phys.*, 3, 181–193, doi:10.5194/acp-3-181-2003, 2003.
- Jenkin, M. E., Watson, L. A., Utembe, S. R., and Shallcross, D. E.: A Common Representative Intermediates (CRI) mechanism for VOC degradation. Part 1: Gas phase mechanism development, *Atmos. Environ.*, 42, 7185–7195, 2008.
- Kleinman, L. I.: Seasonal dependence of boundary layer peroxide concentration: the low and high NO_x regimes, *J. Geophys. Res.*, 96, 20721–20733, 1991.
- Kleinman, L. I.: Low and high NO_x tropospheric photochemistry, *J. Geophys. Res.*, 99, 16831–16838, 1994.
- Koss, A. R., de Gouw, J., Warneke, C., Gilman, J. B., Lerner, B. M., Graus, M., Yuan, B., Edwards, P., Brown, S. S., Wild, R., Roberts, J. M., Bates, T. S., and Quinn, P. K.: Photochemical aging of volatile organic compounds associated with oil and natural gas extraction in the Uintah Basin, UT, during a wintertime ozone formation event, *Atmos. Chem. Phys.*, 15, 5727–5741, doi:10.5194/acp-15-5727-2015, 2015.
- Kuhn, M., Bultjes, P. J. H., Poppe, D., Simpson, D., Stockwell, W. R., Andersson-Sköld, Y., Baart, A., Das, M., Fiedler, F., Hov, Ø., Kirchner, F., Makar, P. A., Milford, J. B., Roemer, M. G. M., Ruhnke, R., Strand, A., Vogel, B., and Vogel, H.: Intercomparison of the gas-phase chemistry in several chemistry and transport models, *Atmos. Environ.*, 32, 693–709, 1998.
- Li, J., Georgescu, M., Hyde, P., Mahalov, A., and Moustouli, M.: Achieving accurate simulations of urban impacts on ozone at high resolution, *Environ. Res. Lett.*, 9, 114019, doi:10.1088/1748-9326/9/11/114019, 2014.
- Lidster, R. T., Hamilton, J. F., Lee, J. D., Lewis, A. C., Hopkins, J. R., Punjabi, S., Rickard, A. R., and Young, J. C.: The impact of monoaromatic hydrocarbons on OH reactivity in the coastal UK boundary layer and free troposphere, *Atmos. Chem. Phys.*, 14, 6677–6693, doi:10.5194/acp-14-6677-2014, 2014.
- Rickard, A., Young, J., Pilling, M., Jenkin, M., Pascoe, S., and Saunders, S.: The Master Chemical Mechanism Version MCM v3.2, available at: <http://mcm.leeds.ac.uk/MCMv3.2/>, last access: 15 July 2015.
- Sander, R., Kerkweg, A., Jöckel, P., and Lelieveld, J.: Technical note: The new comprehensive atmospheric chemistry module MECCA, *Atmos. Chem. Phys.*, 5, 445–450, doi:10.5194/acp-5-445-2005, 2005.
- Saunders, S. M., Jenkin, M. E., Derwent, R. G., and Pilling, M. J.: Protocol for the development of the Master Chemical Mechanism, MCM v3 (Part A): tropospheric degradation of non-aromatic volatile organic compounds, *Atmos. Chem. Phys.*, 3, 161–180, doi:10.5194/acp-3-161-2003, 2003.
- Sillman, S.: The relation between ozone, NO_x and hydrocarbons in urban and polluted rural environments, *Atmos. Environ.*, 33, 1821–1845, 1999.
- Stevenson, D. S., Young, P. J., Naik, V., Lamarque, J.-F., Shindell, D. T., Voulgarakis, A., Skeie, R. B., Dalsoren, S. B., Myhre, G., Berntsen, T. K., Folberth, G. A., Rumbold, S. T., Collins, W. J., MacKenzie, I. A., Doherty, R. M., Zeng, G., van Noije, T. P. C., Strunk, A., Bergmann, D., Cameron-Smith, P., Plummer, D. A., Strode, S. A., Horowitz, L., Lee, Y. H., Szopa, S., Sudo, K., Nagashima, T., Josse, B., Cionni, I., Righi, M., Eyring, V., Conley, A., Bowman, K. W., Wild, O., and Archibald, A.: Tropospheric ozone changes, radiative forcing and attribution to emissions in the Atmospheric Chemistry and Climate Model Intercomparison Project (ACCMIP), *Atmos. Chem. Phys.*, 13, 3063–3085, doi:10.5194/acp-13-3063-2013, 2013.
- Stockwell, W. R., Middleton, P., Chang, J. S., and Tang, X.: The second generation regional acid deposition model chemical mechanism for regional air quality modeling, *J. Geophys. Res.*, 95, 16343–16367, 1990.
- Stockwell, W. R., Kirchner, F., Kuhn, M., and Seinfeld, S.: A new mechanism for regional atmospheric chemistry modeling, *J. Geophys. Res.-Atmos.*, 102, 25847–25879, 1997.
- Watson, L. A., Shallcross, D. E., Utembe, S. R., and Jenkin, M. E.: A Common Representative Intermediates (CRI) mechanism for VOC degradation. Part 2: Gas phase mechanism reduction, *Atmos. Environ.*, 42, 7196–7204, 2008.
- Yarwood, G., Rao, S., Yocke, M., and Whitten, G. Z.: Updates to the Carbon Bond Chemical Mechanism: CB05, Tech. rep., US Environmental Protection Agency, Novato, California, USA, 2005.

Chapter 7

Paper 2:

Chapter 8

Paper 3:

Chapter 9

Publication List

Appendix

